Late Pleistocene Glacial History and Reconstruction of the Fish Lake Plateau, South-Central Utah: Implications for Climate at the Last Glacial Maximum

Sarah C. Bergman
Senior Integrative Exercise
March 9, 2007

Submitted in partial fulfillment of the requirements for a Bachelor of Arts degree from Carleton College, Northfield, Minnesota.

TABLE OF CONTENTS

Late Pleistocene Glacial History and Reconstruction of the Fish Lake Plateau, South-Central Utah: Implications for Climate at the Last Glacial Maximum

Sarah C. Bergman
Carleton College
Senior Integrative Exercise
March 9, 2007

Advisors:
Mary Savina, Carleton College
Chuck Bailey, College of William & Mary
Dave Marchetti, Colgate University

Abstract

The Fish Lake Plateau (2700 – 3500 m; south-central Utah) experienced at least two episodes of Pleistocene glaciation. The geographic extent of eight, late Pleistocene paleoglaciers (Last Glacial Maximum - LGM) were determined through field mapping as well as topographic map and aerial photography interpretation. Paleoglaciers are reconstructed with spreadsheet models that generate glacier longitudinal profiles constrained by bedrock morphology, moraine crest elevations, basal shear stress and shape factor. Equilibrium-line altitudes (ELAs) are determined for reconstructed glaciers with accumulation-area ratio, toe-to-headwall-altitude ratio, maximum altitude of lateral moraines, and cirque floor altitude methods. ELAs respond directly to climate variations, and the difference between modern and Pleistocene ELAs is used as a proxy for climate change. Direct measurement of modern ELAs is not possible because Utah is not currently glaciated. Regression to the July 0º C isotherm from local climate data with an assumed atmospheric lapse rate of 6º C/1 km indicates a 4900 m modern ELA. ELAs for Fish Lake paleoglaciers range from 2950 to 3250 m, a depression of 1650 to 1950 m from modern levels.

General circulation models suggest a colder, drier LGM climate in the western U.S. If ELA depression is attributed solely to summer temperature depression, the measured depression corresponds to a 10 to 12º C lowering of LGM summer season temperatures. This temperature depression is likely overestimated, however, little is known about possible lake enhancement from glacial Lake Bonneville on LGM precipitation regimes of south-central Utah. Regardless of uncertainties due to the dynamic relationship between temperature, precipitation, and their combined effect on glacier mass balance, the ELA depression in southern Utah measured in this study suggests LGM summer temperatures were around 10º C cooler than modern values on the Fish Lake Plateau.

Keywords: glaciers, last glacial maximum, Pleistocene, paleoclimate, Lake Bonneville, Utah

INTRODUCTION

Cyclical alterations between glacial and interglacial climate due to changes in incoming solar radiation (insolation) characterize the Quaternary Period of Earth history (1.6 Ma – present; Benn and Evans, 1998). The Last Glacial Maximum (LGM) occurred approximately 21 ka and corresponds to the maximum extent of the Cordilleran and Laurentide Ice Sheets (Fig. 1; Mickelson et al., 1983). During this time the 3000 m thick Laurentide Ice Sheet extended across central Canada, splitting the polar jet stream and altering atmospheric circulation patterns and moisture sources throughout North America (COHMAP Members, 1988). Late Pleistocene landscapes and surficial processes differed significantly from present conditions as a result of these changes. Throughout the western United States, maximum alpine glacial ice extent was primarily synchronous with the LGM (e.g. the Pinedale glaciation, Wind River Range, Wyoming; Chadwick et al., 1997). Late Pleistocene timing of the maximum extent of western mountain glacier systems varied in space, occurring between 21-18 ka (Munroe et al., 2006). The temporal variability between maximum alpine glacier extent and the LGM varies because temperature and precipitation levels dictate the conditions under which glaciers exist. Thus, spatial variations in atmospheric circulation patterns lead to cold, wet, glacially favorable conditions in certain regions and more arid environments in others.

Cool summers and precipitation-heavy winters characterize the LGM climate of the southwestern United States (Thompson et al., 1993; Galloway, 1970). Alternately, cool summers and decreased precipitation levels exemplify late Pleistocene climatic patterns for the northern U.S. (Hostetler and Clark, 1997; Locke, 1990; Porter et al.,

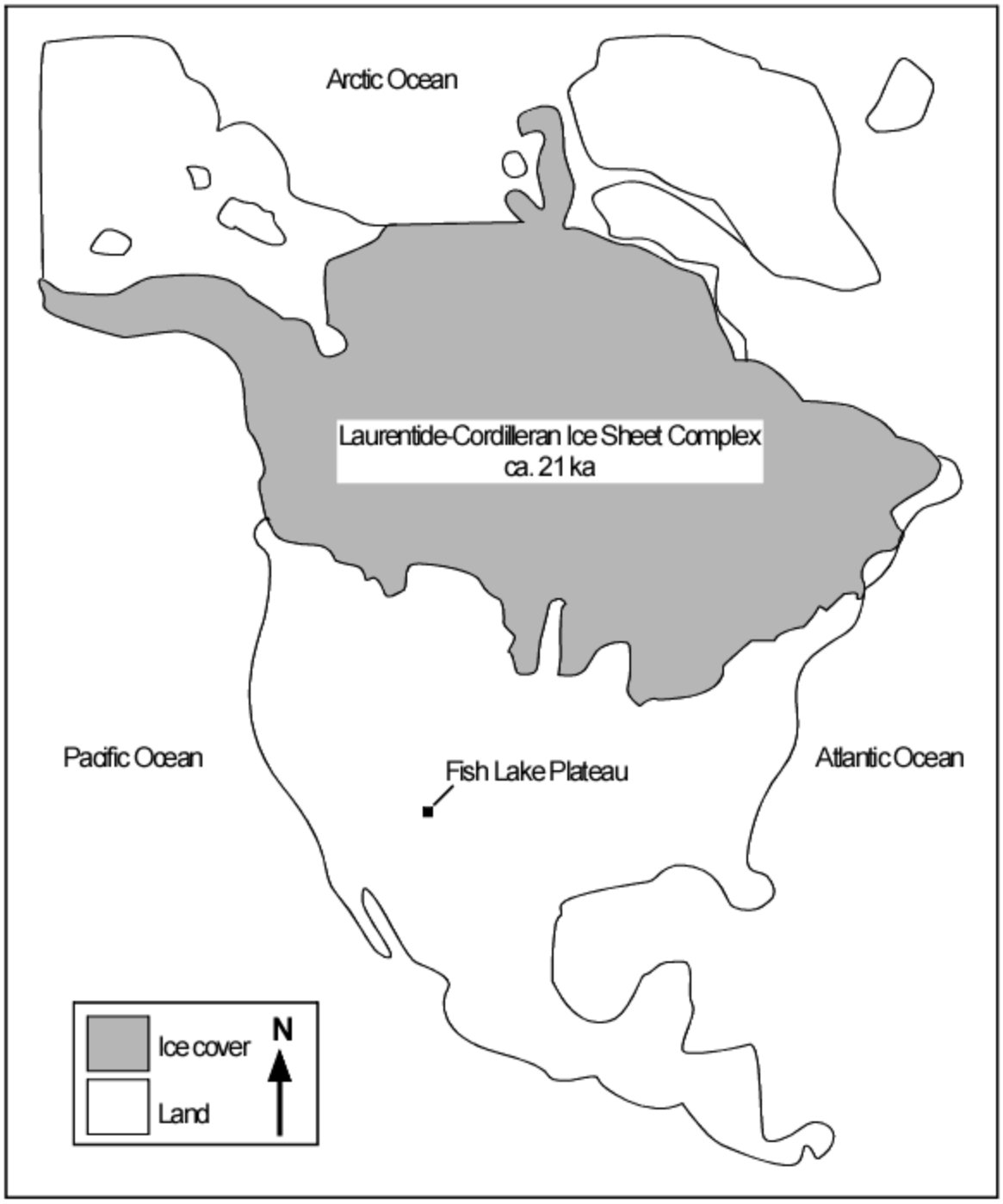

Figure 1. Extent of the Laurentide-Cordilleran Ice Sheet complex at the Last Glacial Maximum (21 ka). Modified from Beaudoin et al., as compiled by Adams (2007).

1983; Thackray, 2004). These climate patterns led to the development and maintenance of late Pleistocene alpine glacier populations from Montana to New Mexico (Fig. 2).

Climatic conditions conducive to limited glaciation, albeit with warmer summer season temperatures than during the LGM, still exist in the northern Rocky Mountains and the Pacific Northwest. Modern alpine glacier populations are found in Montana, Idaho, Wyoming and the Cascade Range (Locke, 1989; Porter, 1977). Late Pleistocene glaciations in these areas are relatively well studied (e.g. Brugger, 2006; Brugger and Goldstein, 1999; Licciardi et al., 2004; Meierding, 1982; Murray and Locke, 1989; Zwick, 1980). Thus, comparison between past and present conditions of glaciated regions is possible. This increases understanding of alpine glacial mechanics and the climate conditions favorable to LGM glaciation at mid-high latitudes in North America.

However, global climate change and the collapse of the Laurentide Ice Sheet at the last glacial termination prevent comparison between late Pleistocene climate and modern analogues in the southwestern United States. In contrast to its modern state of aridity, alpine glaciation, cool summer temperatures and glacial Lake Bonneville characterize LGM climate and landscape in the Intermountain West, the region between the Sierra Nevada and the Rocky Mountains (Hostetler et al., 1994; Galloway, 1970).

Little is known regarding the nature, extent or hydrologic controls on LGM glaciation in the American Southwest. In a localized study of alpine paleoglaciation in south-central Utah, I reconstruct late Pleistocene glaciers on the Fish Lake Plateau (Fig. 3). This region is not currently glaciated, however, at the LGM at least eight small, alpine glaciers existed on the Plateau (Fig. 4). Glacial mapping and reconstruction of this region places further constraints on the nature of late Pleistocene, alpine glaciation in the

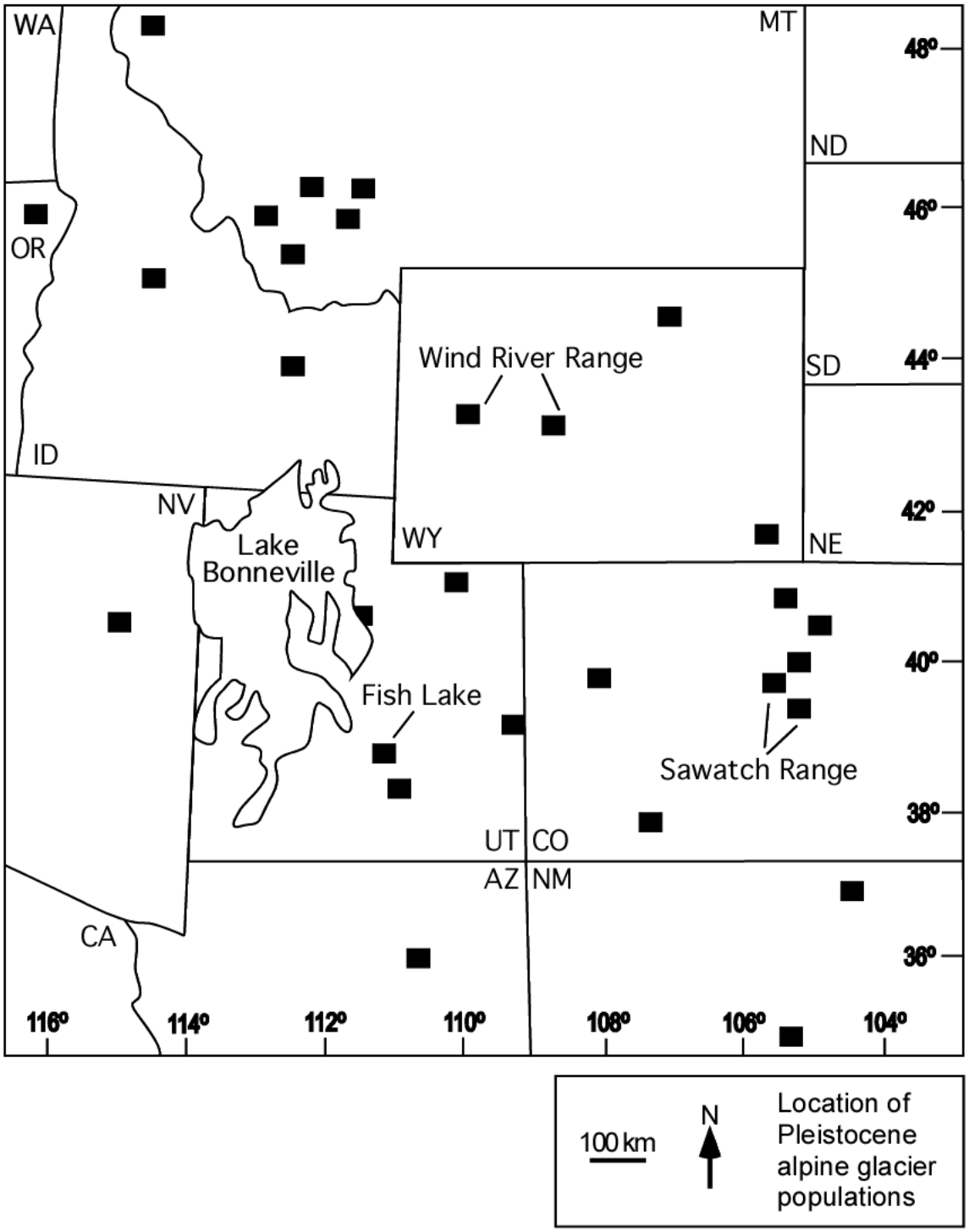

Figure 2. Location of late Pleistocene alpine glacier populations in the Rocky Mountains and the Intermountain West. Modified from Webber (2003) and Hostetler et al. (1994).

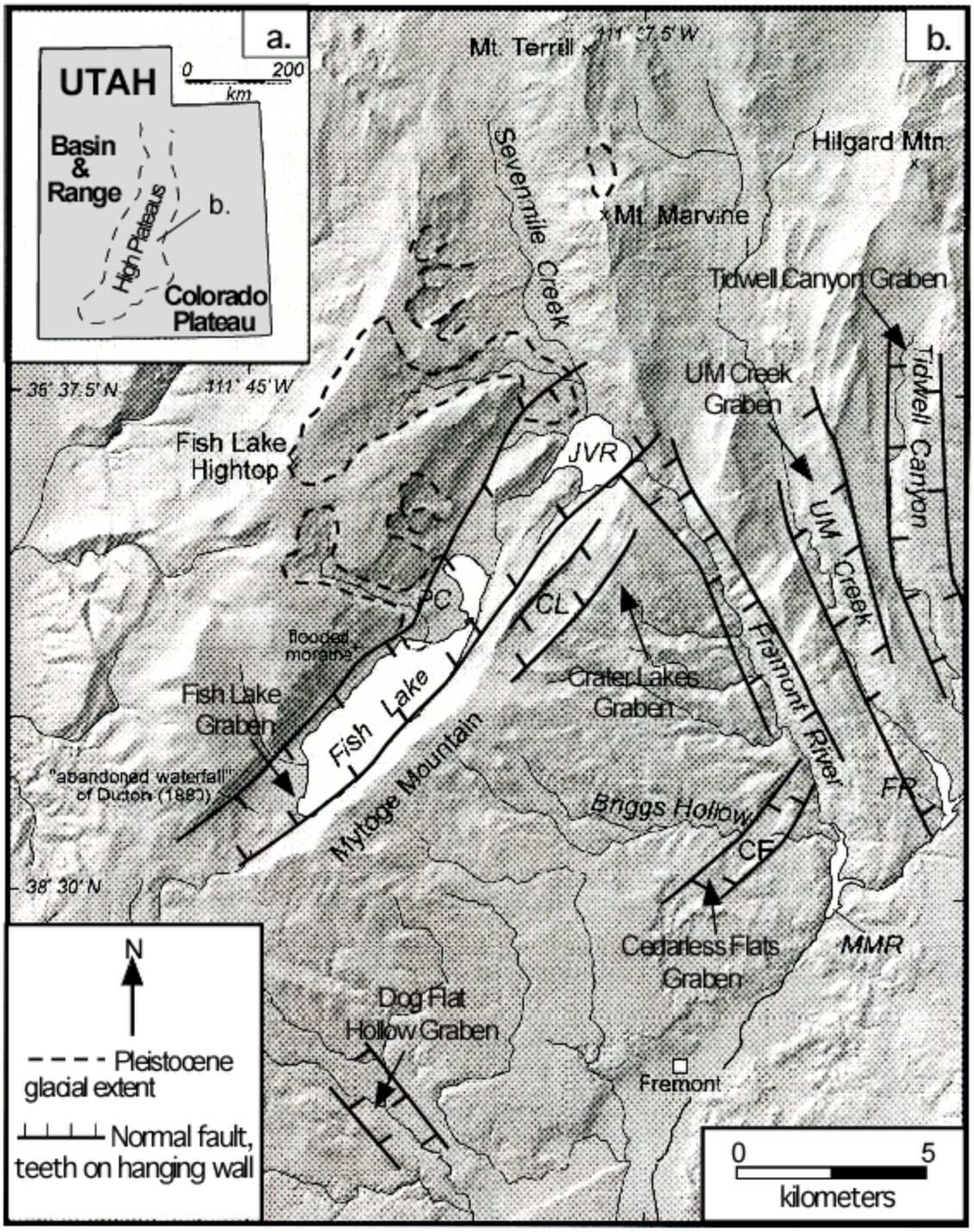

Figure 3. Site map of the Fish Lake Plateau; a. Map of Utah; b. Detail of the Fish Lake Plateau. Prominent structural and geomorphologic features are marked. Modified from Bailey et al. (2007).

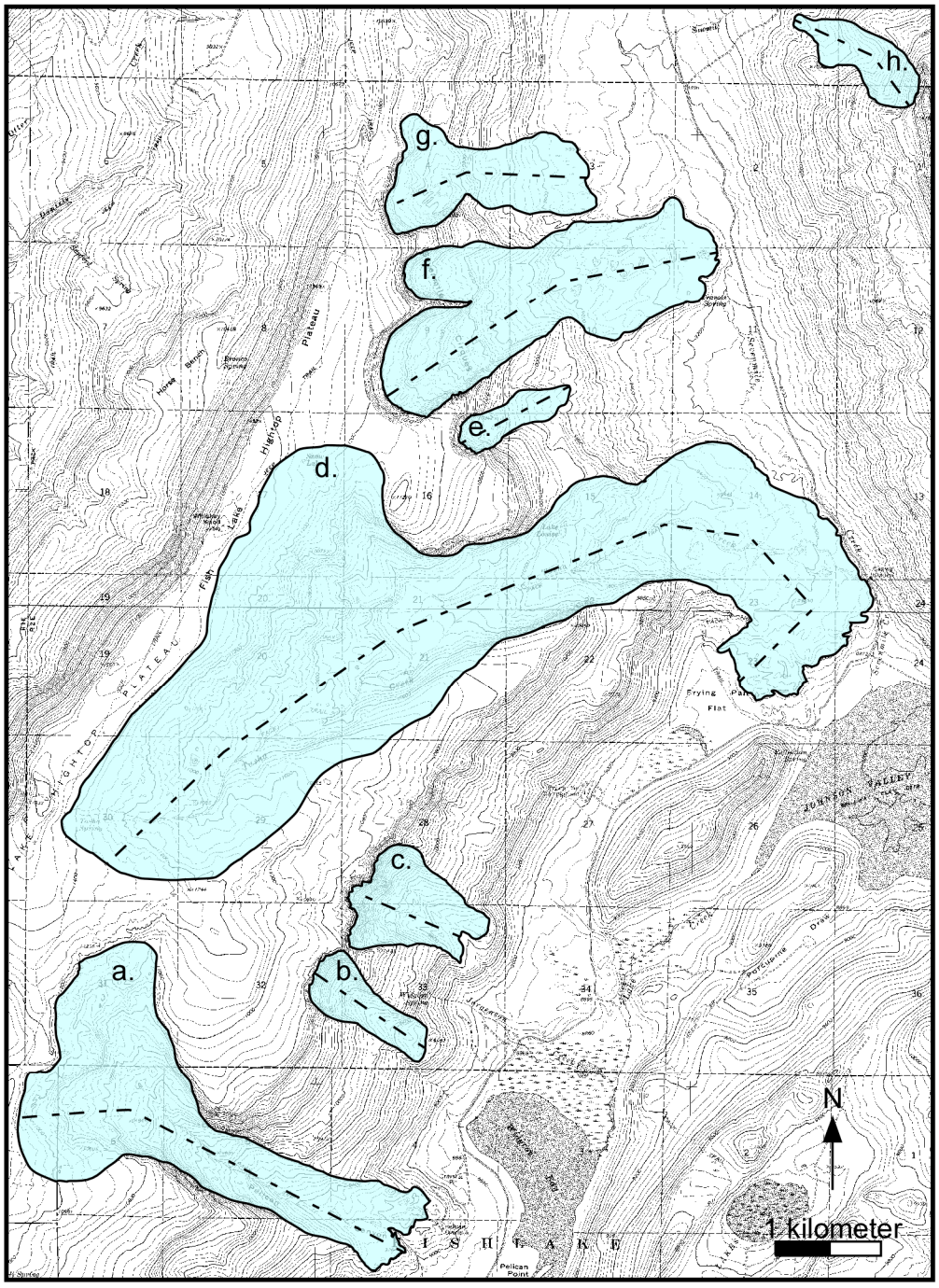

Figure 4. Location and geographic boundaries of LGM paleoglaciers on the Fish Lake Plateau. a. Pelican Canyon; b. Jorgenson Cirques South; c. Jorgenson Cirques North; d. Tasha Creek; e. Seven Mile Cirques South; f. Seven Mile Cirques Center; g. Seven Mile Cirques North; h. Mount Marvine. Dashed line denotes the centerline path used in GlacPro glacial reconstruction. For paleoglaciers with multiple lobes and cirque-like features, the centerline follows the features that indicate the greatest ice volume, as identified by surficial deposits and erosional landforms in field mapping. Modified from the Fish Lake and Mount Terrill 7.5-minute series quadrangle maps (U.S. Geological Survey, 2001).

southern Intermountain West. This information, in conjunction with glacial reconstruction studies from the Rocky Mountains and the Pacific Northwest broadens current understanding of the dynamics of late Pleistocene glaciations throughout the western United States (Leonard, 1984, 1989; Meierding, 1982; Porter, 1977; Licciardi et al., 2004).

CLIMATE HISTORY

ORBITAL FORCING

Fluctuations between glacial and non-glacial climates exemplify the Quaternary Period. Cyclical changes in the Earth's orbit around the sun, known as Milankovitch cycles, drive these fluctuations (Benn and Evans, 1998). The three known Milankovitch cycles are eccentricity, precession and obliquity. Eccentricity is a measure of the degree of ellipticity of the Earth's orbit and occurs on a 100,000 year cycle. Obliquity, a measure of the tilt of the Earth's rotational axis relative to the orbital plane, fluctuates on a 41,000 year cycle. Precession is a 23,000 year cycle of the direction of tilt of the Earth's axis relative to the stars (Benn and Evans, 1998). Variations in seasonality and insolation due to fluctuations in these orbital cycles lead to the development of positive feedback cycles in the climate system. These cycles cause oscillations between glacial and interglacial periods.

THE LAST GLACIAL MAXIMUM

The last glacial period occurred in the late Pleistocene. The maximum extent of ice sheets and glaciation during this cycle corresponds to the Last Glacial Maximum, 21 ka. The Laurentide Ice Sheet that covered the majority of North America at this time was at least 3000 m thick and heavily influenced atmospheric circulation and precipitation

patterns in what is now the United States and Canada. General circulation models suggest that polar jet stream dynamics differed significantly at the LGM as a result of ice sheet geometry (COHMAP Members, 1988). The authors hypothesize that the Laurentide Ice Sheet split the polar jet stream, which displaced an arm southward, leading to increased precipitation in the American Southwest (Fig. 5). In contrast, they find that easterly winds, driven by the glacial anticyclone over Canada, developed immediately to the south of the Laurentide Ice Sheet. This initiated significantly drier conditions in the Pacific Northwest. Variations on decreased temperature and increased precipitation conditions in the contiguous U.S. led to the development of LGM alpine glacier systems throughout the Rocky Mountains and the western United States. Although the maximum extent of ice in these mountain glacier systems varied in time throughout the United States, it was broadly synchronous with the maximum extent of the Laurentide Ice Sheet 21 ka. The late Pleistocene paleoglaciers reviewed in this study are considered LGM-era due to their coeval development with Laurentide Ice Sheet transgression between 21-18 ka, and age correlation with the Pinedale glaciation of the Wind River Range, Wyoming from cosmogenic nuclide dating (c.f. Weaver et al., 2006).

GLACIERS AND GLACIATION

ALPINE GLACIERS

Glaciers constitute approximately 1.7% of the Earth's water in storage. Total ice volume is divided between the Antarctic Ice Sheet, the Greenland Ice Sheet, mountain glaciers and small mountain ice caps (Van der Veen, 1999). Glaciers are divided into two categories: alpine-type glaciers and ice sheets. Ice sheets are large masses of ice found in high northern and southern latitudes. Continental ice sheets are up to hundreds

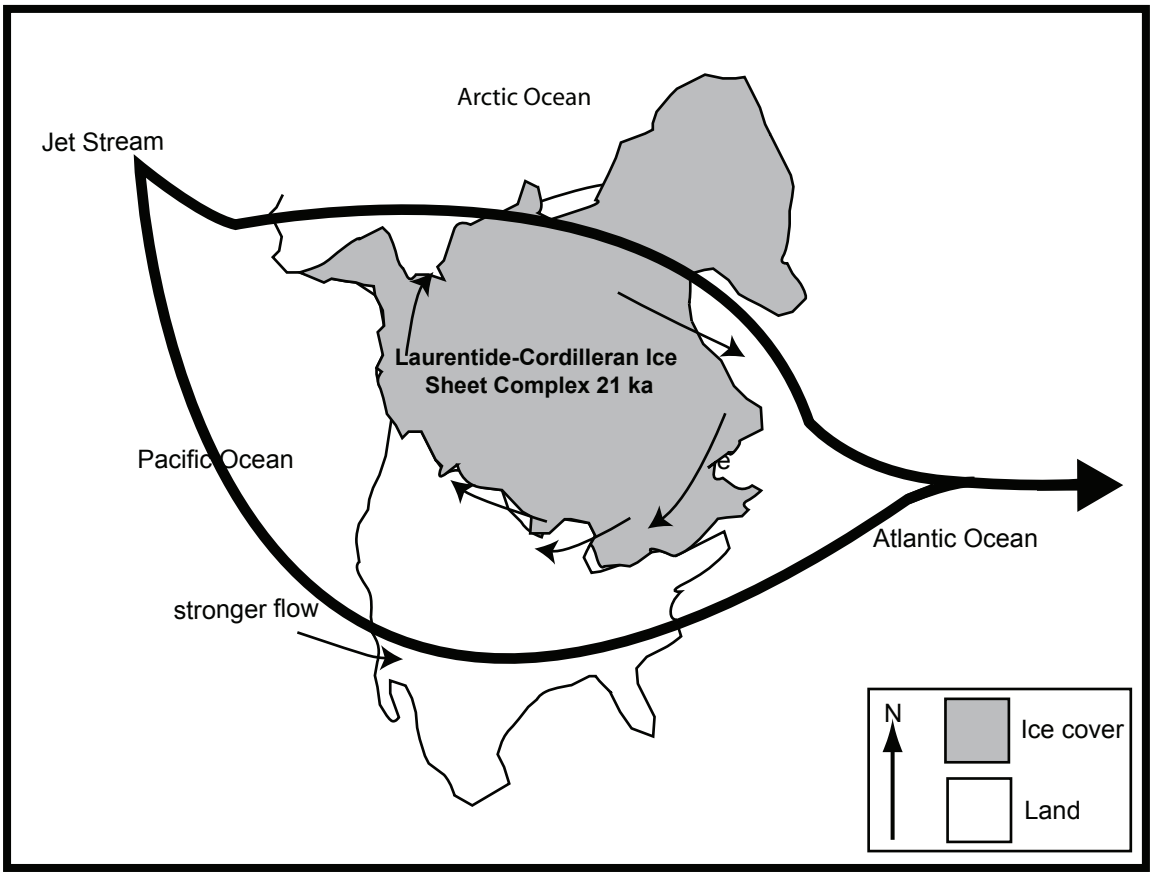

Figure 5. Suggested path of a split polar jet stream over North America during the late Pleistocene from General Circulation Models. The path splits as it moves over the Laurentide and Cordilleran Ice Sheets, directing an arm southward. Conditions are colder and drier immediately to the south of the glacial anticyclone; conditions are colder and wetter along the southern path of the jet stream. The Fish Lake Plateau falls between these two zones. Modified from COHMAP Members (1988).

of kilometers in area, and multiple kilometers thick. Ice sheets form during glacial cycles, and significantly impact both regional and global climate cycles and circulation patterns (Van der Veen, 1999).

In contrast to ice sheets, alpine glaciers are small ice masses found in high mountain environments (Fig. 6). Unlike ice sheets, kilometer-scale alpine glaciers do not constitute a great enough portion of the Earth's water budget to appreciably alter global climate patterns. Small mountain glaciers are heavily influenced, and even controlled by regional trends in climate and geography. Local topography; aspect, which is the cardinal direction a glacier faces; and microclimate largely determine glacial development in alpine environments (Benn and Evans, 1998; Van der Veen, 1999). Due to the recession of the Laurentide Ice Sheet and the current interglacial climate, present-day glaciation in the contiguous United States is limited to a network of small alpine glacier systems in the Rocky Mountains and the Cascade Range of the Pacific Northwest.

Alpine glaciers develop in a variety of characteristic shapes. Hooke (2005) discusses the general morphology of alpine glaciers. The most common glacier forms are valley and cirque-shapes. U-shaped, valley glaciers are long, relatively narrow ice masses, which move under unidirectional flow. Their paths are constrained by valley or canyon walls. Glaciers that occupy mountain basins are called cirque glaciers (Fig. 6). These ice masses sit in and carve out bowl-like depressions in high mountain regions. In addition to mountain glaciers, Hooke (2005) also discusses the morphology of ice caps. Ice caps are small, dome-like glaciers that spread in any direction from a topographic high. Ice caps often form on plateaus and gently sloping mountain summits.

Figure 6. Receding modern cirque and valley glaciers in the Chugach Mountains, Alaska. Dotted line denotes the glacier terminus. Modified from a photograph by Bruce Molnia, U.S. Geological Society (2007).

Van der Veen (1999) identifies mountain glaciers' and small ice caps' susceptibility to both large-scale variations in climate, and more local environmental changes. Glaciers respond rapidly to climate change, and small, mid-high latitude temperate glaciers are particularly good indicators of that change on the decadal scale (Porter, 1986). Additionally, alpine glaciers differ from ice sheets in their sensitivity to temperature versus precipitation. Continental ice sheets respond primarily to changes in winter season precipitation, while alpine glaciers are heavily influenced by variations in summer season temperature (Hostetler and Clark, 1997).

GEOMORPHIC INDICATORS OF GLACIATION

Glaciers and ice sheets flow by internal deformation and sliding due to gravity (Benn and Evans, 1998). This deformation transfers snow and ice from accumulation areas to ablation areas, resulting in glacial erosion and debris transport (Benn and Evans, 1998). As a result of deposition and erosion, glacier movement creates significant geomorphic and topographic features at both glacier termini and headwalls.

Moraines are ice-marginal features that develop at the lower limits of glaciers. Glaciers erode debris from their bases and transfer it to their termini, where the debris forms steeply angled ridges at the toe and lateral edges of alpine glaciers. Moraine crest elevation generally matches ice surface elevation at the glacier terminus (Fig. 7; Benn and Evans, 1998). Moraines are particularly useful to glacial reconstruction because moraine position corresponds to a glacier's boundaries at a specific point in time. Thus, moraine location is a record of both glacier terminus position in geographic space and ice surface elevation at the terminus.

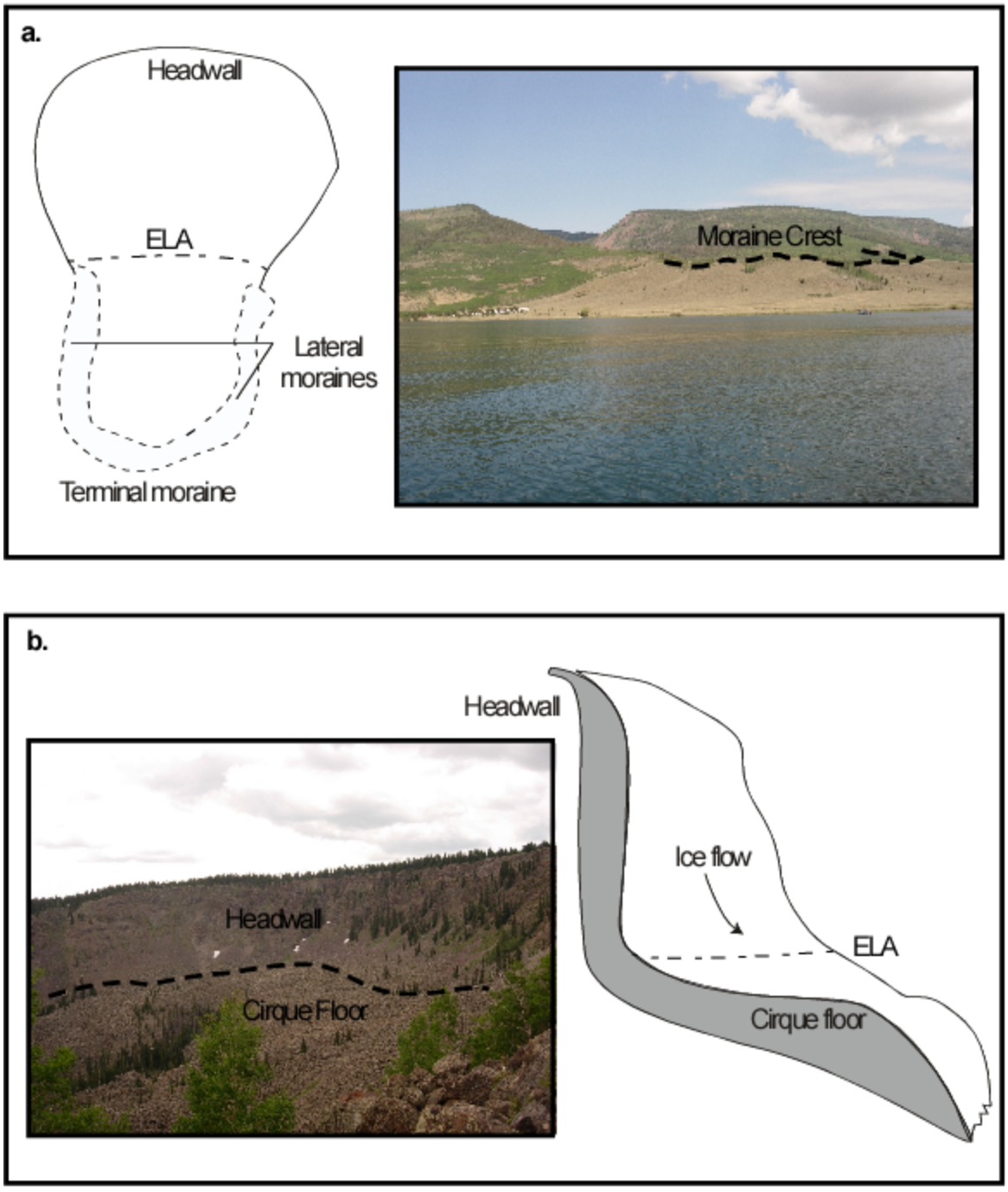

Figure 7. a. Map view of a cirque or valley glacier with lateral and terminal moraines, and ELA; photograph of the terminal moraine at Pelican Canyon, Fish Lake, Utah; b. Cross section of a cirque glacier in a mountain basin with marked ELA; phoograph of cirque headwall and floor from the Seven Mile Cirques, Fish Lake, Utah. Personal photographs (2006).

GLACIER DYNAMICS

Glaciers develop when winter snow accumulation in a region exceeds summer water loss, resulting in the progressive burial of snow. Over time, individual snow layers are compacted by pressure due to burial. This buried snow metamorphoses into ice over several years. A glacier is formed when the metamorphosed ice mass is thick enough to flow under its own weight (Hooke, 2005).

Glaciers are divided into two regions, the accumulation and ablation zones. Glaciers grow by the addition of snow and ice to the upper accumulation zone. Mass loss through melting, sublimation and calving of glaciers in bodies of water occurs in the lower ablation zone. The glacier equilibrium-line altitude (ELA) separates the accumulation and ablation zones. The ELA is the line on the surface of a glacier where net mass balance equals zero (i.e. input matches loss; Fig. 8).

Glacier mass balance responds directly to both large and small-scale variations in climate. Thus, ELA position is a function of the particular temperature and precipitation regime in a given glacier location. Equilibrium-line altitude is also a function of glacier aspect and local topography, which strongly influence alpine glacier morphology (Benn and Evans, 1998). South and east-facing glaciers generally have higher ELAs because they receive more exposure to sunlight and solar radiation than north and west-facing glaciers. Accumulation zone area decreases with increasing exposure to solar radiation, which directly affects glacier melting and water loss rates.

North and northwest-facing glaciers in North America generally receive more precipitation than south and southeast-facing glaciers, effectively lowering their ELAs. Prevailing storm tracks from the Pacific coast increase precipitation on glaciers with west

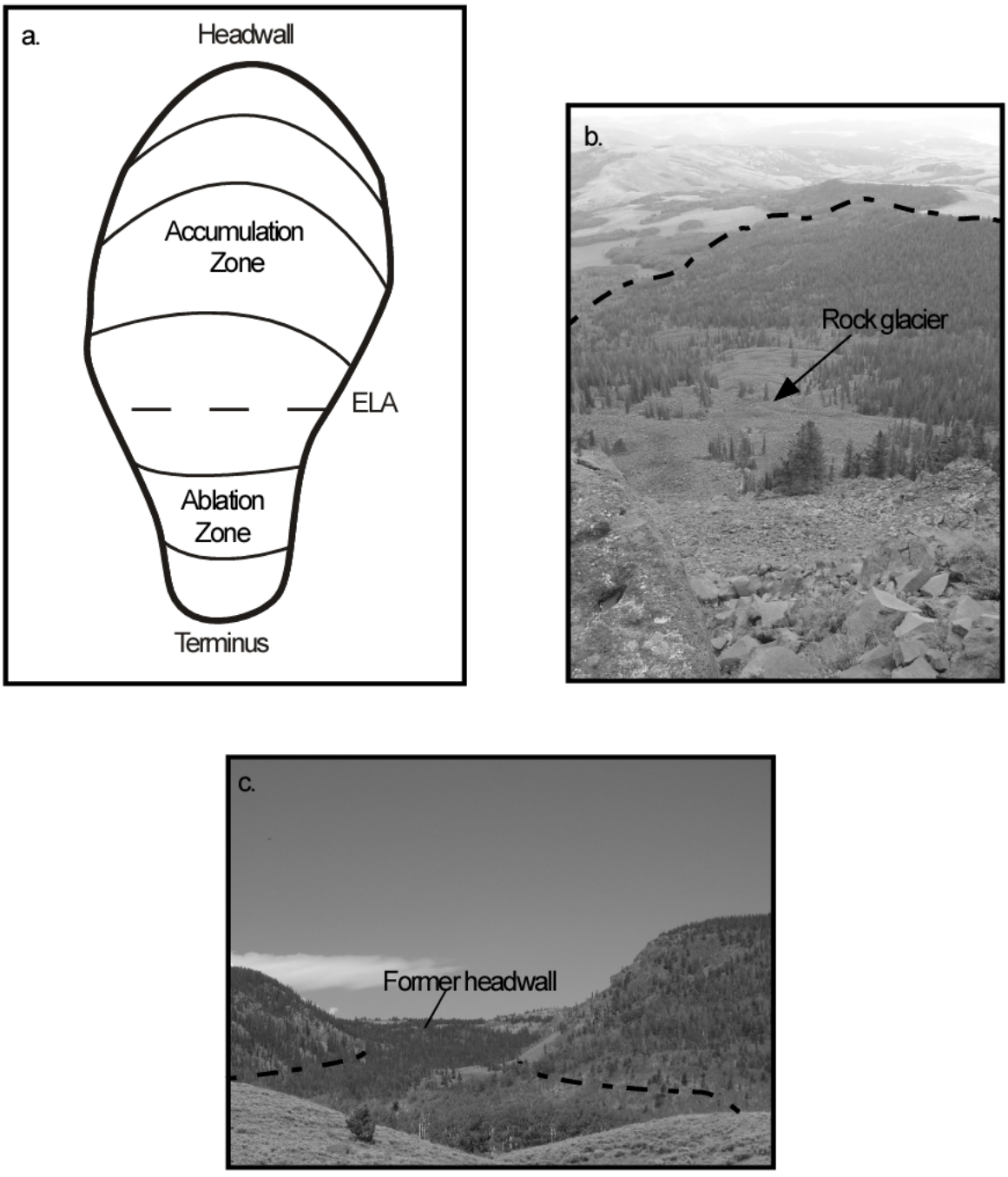

Figure 8. a. Schematic diagram of an alpine glacier in map view. The accumulation zone is at a higher elevation than the ablation zone; b. remnant of a rock glacier, Mount Hilgard. Terminal moraines in tree cover are denoted by the dashed line; c. Pelican Canyon. Dotted lines denote the valley the Pelican Canyon paleoglacier flowed through at the LGM. The former headwall of the glacier is located in the center of the photograph. Photographs from personal collection (2006).

and northwest aspects. Orographic effects on dominantly north-south trending mountain ranges create a rain shadow effect on the eastern flanks of these ranges, which also decreases precipitation for glaciers with eastern aspects. Topography has a similar localized effect on ELA. Glaciers that receive significant shading due to relief have lower ELAs than non-shaded glaciers because they receive lower levels of solar radiation.

ELAs for individual glaciers, as well as regional ELAs, often differ significantly from year-to-year due to annual variations in temperature and precipitation. However, the regional steady-state ELA associated with zero mass balance is a good indicator of regional climate. Studies of modern glacial environments show that fluctuations in glacier mass balance are strongly correlated for glaciers within 500 km of one another (Letreguilly and Reynaud, 1989). These regional ELAs, which are located at the average altitude for steady-state zero mass balance conditions within a 500 km area, correspond to the regional, mean July 0º C isotherm (Porter, 1977). The elevation of the mean July freezing isotherm determines the location of a glacier's ablation and accumulation zones during the summer season. For modern alpine glacier systems ablation season temperature has a greater influence than winter season precipitation on mass balance, thus the July 0º C isotherm is analogous to the ELA.

Correlation of the equilibrium line with a specific temperature (i.e. the mean July or summer 0º C isotherm) allows geologists to use elevation differences in regional ELAs through time as a proxy for continental climate change. Reconstruction of eight, late Pleistocene alpine glaciers on the Fish Lake Plateau yields estimates for LGM equilibrium-line altitudes in south-central Utah. Comparison of ELAs for reconstructed

paleoglaciers with modern ELAs provides preliminary estimates for LGM ELA depressions and summer temperature depressions in the Intermountain West.

STUDY AREA

The Fish Lake Plateau, south-central Utah (38° 36' N; 111° 44' W), is one of the High Plateaus of Utah, which separate the Colorado Plateau from the Basin and Range province of the western United States. Fish Lake Plateau is approximately 1500 km^2 in area. The Plateau ranges in elevation from 2700 m (8,843 feet) in the Fish Lake basin to 3547 m (11,633 feet) on the Fish Lake Hightop. The Fish Lake Plateau is bounded by the Fish Lake Hightop to the west; by Mt. Terrill, Mt. Marvine and Hilgard Mountain to the north; and by Mytoge Mountain to the southeast (Fig. 3).

The Fish Lake Plateau is underlain by a sequence of Oligocene to Pliocene volcanic deposits, which unconformably overlie Cretaceous to early Tertiary sediments (Hardy and Muessig, 1952). The volcanic units are a 250 – 700 m thick series of breccias, trachytes, trachyandesites and olivine basalts, some of which are correlated to defined units of the Marysvale Volcanic field to the west (Fig. 9; Bailey et al., 2007; Hardy and Muessig, 1952). Informal names are used in the stratigraphic column for units unique to the Fish Lake area.

Sandstones and conglomerates unconformably overlie volcanic units in the Fremont and Upper Moroni (UM) Creek basins in the northeastern section of the Fish Lake Plateau (Bailey et al., 2007). Quaternary surficial deposits including glacial till and outwash, boulder-armored terrace deposits, lacustrine and marsh deposits, debris flow, slump, colluvial deposits and alluvium are found throughout the Fish Lake Plateau at

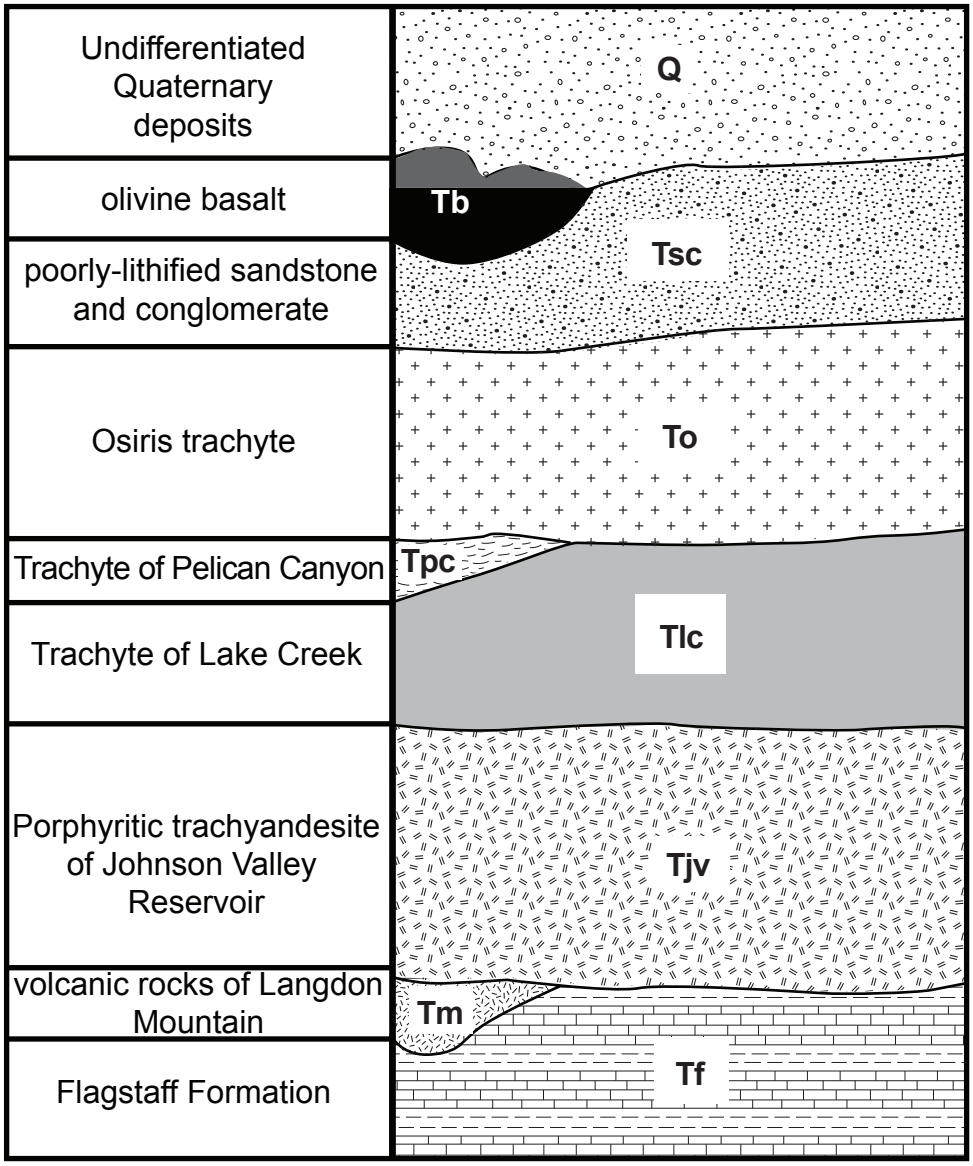

Figure 9. Stratigraphic column of the Fish Lake Plateau.

Cedarless Flats, UM Creek, the Fremont River Graben, Tidwell Canyon and the Fish Lake Graben (Bailey et al., 2007; Fig. 3).

GEOLOGIC SETTING

Fish Lake has a complex tectonic history characterized by multiple generations of Pliocene to Pleistocene normal faulting. Bailey et al. (2007) identify structural features and constrain the timing of faulting on the Fish Lake Plateau. Tertiary sediments and volcanic rocks are cut by multiple generations of steeply-dipping, crosscutting, normal faults. These faults result in north-northwest and northeast trending horst-and-graben topography. Northwest trending faults form grabens along the Fremont River, UM Creek, Cedarless Flats, Crater Lakes and Tidwell Canyon (1-5 Ma). Fish Lake itself occupies a younger, northeast trending graben ($\leq$ 900 ka; Fig. 3; Fig. 10; Dickson et al., 2006).

The Fish Lake Plateau was glaciated at least twice during the Pleistocene. Weaver et al. (2006) sampled large, morainal Johnson Valley Reservoir trachyte boulders for cosmogenic ^{3}He in the summer of 2005. Their results yield two glacial age groupings, which correspond to the Bull Lake (186-128 ka) and Pinedale (24-12 ka) glaciations of the Wind River Range, Wyoming. Tasha Creek paleoglacier samples yield an age of 135 $\pm$ 4 ka. Dates from Pelican Canyon, Jorgenson Cirques, Tasha Creek and Seven Mile Cirques yield ages between 21.1 $\pm$ 2.2 to 23.2 $\pm$ 3.7 ka.

COSMOGENIC ^{3}HE EXPOSURE AGE DATING

Cosmogenic isotopes produced in rocks are used to date the age of geomorphic surfaces, including terminal and lateral moraines. Cosmogenic nuclide exposure age

Figure 10. Photographs of prominent grabens on the Fish Lake Plateau. Dotted lines indicate contaact between graben fill and estimated fault planes. a. Fish Lake graben; b. UM Creek graben; c. Tidwell Canyon graben.

dating derives from the principle that as cosmic rays bombard terrestrial materials cosmogenic nuclides develop near their surfaces (Cerling and Craig, 1994; Fig. 11). Cosmogenic nuclides are isotopes produced in rocks, sediments and other earth materials by the interaction of cosmic nuclei with atoms in the atmosphere and their subsequent spallation reactions with atoms at or near the Earth's surface (Titayeva, 1994). Cosmic rays enter the atmosphere and collide with nuclei, causing a torrent of high-energy neutrons and muons to fall to the earth's surface. The collision between these particles and target nuclei within terrestrial minerals causes spallation reactions and the creation of in-situ produced cosmogenic nuclides in rocks and soils at the earth's surface (Walker, 2005).

Cosmogenic nuclide production rates depend on a number of factors including geomagnetic coordinates, strike, dip, altitude, and erosion and sedimentation rates at the production site (Cerling and Craig, 1994). If the effect of these factors on the rate of cosmogenic isotope production for a specific element and location is known, it is possible to calculate a material's exposure time to cosmic radiation. This directly corresponds to the material's exposure at the surface (Walker, 2005). Thus, exposure age dating provides a quantitative method to determine the geochronology of surficial processes.

Cosmogenic nuclide exposure age dating is particularly useful in Fish Lake to differentiate between multiple generations of Pleistocene glaciation. Exposure age dating was used to correlate the paleoglaciers in the Fish Lake area to the same glacial phase because accurate LGM glacier reconstruction requires quantitative differentiation between episodes of Pleistocene glaciation.

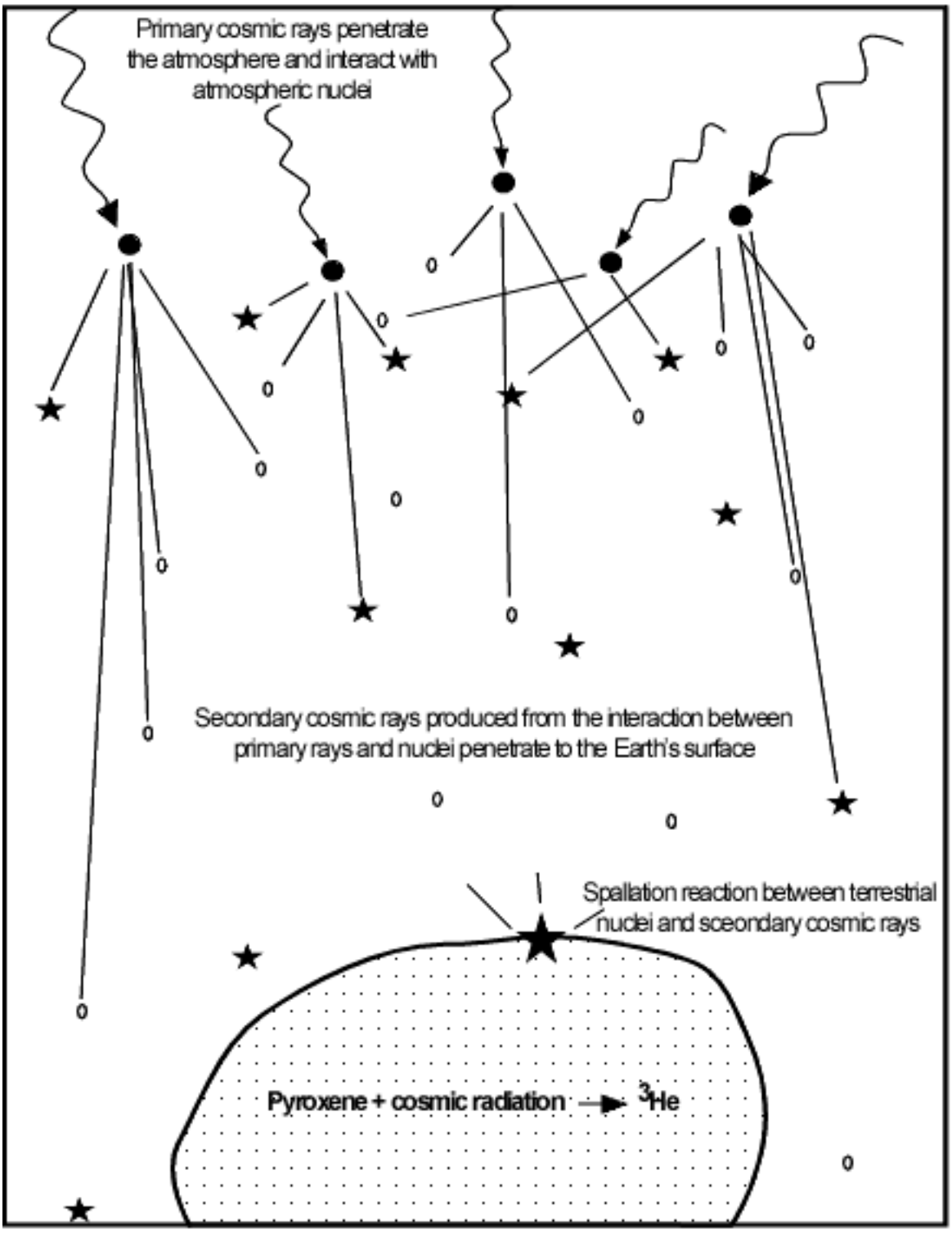

Figure 11. Schematic diagram of cosmogenic ^{3}He production in a boulder. Cosmic rays enter the atmosphere, where collision with nuclei triggers a cascade of high-energy neutrons and muons. These secondary particles collide with nuclei in minerals in terrestrial materials, such as rocks to produce unique nuclides (in situ produced cosmogenic nuclides).

Fish Lake cosmogenic exposure age dating samples were obtained from large, Johnson Valley Reservoir trachyte boulders perched on moraine crests. I sampled boulders greater than one meter in diameter with abundant pyroxene phenocrysts. Samples were chosen based upon rock type, sample size and proximity to moraine crest. These sample selection parameters were employed for a number of reasons. I sampled the Johnson Valley Reservoir trachyte because it is rich in pyroxene phenocrysts, from which cosmogenic ^{3}He is measured. The largest possible boulders were used in order to ensure that a measurable quantity of cosmogenic nuclides have been generated by spallation reactions in the sample. I sampled boulders from moraine crests to ensure that they had not moved since the glaciers receded, thus guaranteeing a maximum exposure age. If a boulder moves after emplacement, the exposure age calculated does not reflect the actual time the sample has been at the surface, but only the exposure time since the boulder's last movement. The true exposure age of a moraine surface must be calculated from samples that have remained stationary since the onset of glacier recession. In addition to these parameters, boulders showing pitting and spalling were not selected for sampling because these conditions indicate that exposure surfaces have been removed. Therefore, these types of samples provide underestimates of surface exposure age.

METHODS

Samples were removed from the top 1-2 inches of large boulders with a hammer and chisel. Latitude, longitude and elevation were recorded from a handheld GPS receiver. Boulder characteristics such as dimensions and shape, as well as tree cover at the sample location were also noted. Shading angle from the surrounding topography

was measured with a clinometer (Fig. 12). Sample locations were recorded on topographic maps and correlated to outlined paleoglacier moraine locations.

Samples were pulverized in a rock crusher, and with a mortar and pestle. Crushed samples were sieved to between 20 – 40 microns. Dave Marchetti did magnetic separation and further sample preparation at the University of Utah Noble Gas Laboratory in 2005 and 2006. The Mount Marvine samples I prepared in 2006 have not been analyzed, however, I hypothesize that all Fish Lake glacial moraines correspond to the LGM, Pinedale-era glaciation. Moraine slope angles from Mount Marvine correspond to those of the seven known Pinedale-era (LGM) moraines on the Fish Lake Plateau measured by Weaver et al. (2006). This geometric similarity in moraine slope angle indicates that the Mount Marvine paleoglacier corresponds to the LGM glaciation of the Fish Lake Plateau.

GLACIAL RECONSTRUCTION

I reconstructed late Pleistocene glaciers in order to quantify LGM ELA depression in south-central Utah. I identified Pinedale-era paleoglaciers with 7.5-minute series, 1:24,000 USGS topographic maps and aerial photography interpretation, as well as field investigation of glacial filling and surficial deposits. Glacier boundaries were outlined on the Fish Lake and Mount Terrill 7.5-minute series quadrangle maps from Sevier County, Utah produced by the U.S. Geological Survey (Fig. 13; 2001). Surficial deposits used to identify glacial boundaries included terminal and lateral moraines, glacial outwash, glacial till, and roche moutonées. Moraine crests marked the boundaries of glacier termini, while valley walls, canyon walls and cirque headwalls served as glacial boundaries up-ice from these termini.

Figure 12. a. Field sampling for cosmogenic ^{3}He nuclides with Dave Marchetti of Colgate University. The sample is a large, Johnson Valley Reservoir trachyte boulder from the UM Creek region of the Fish Lake Plateau.

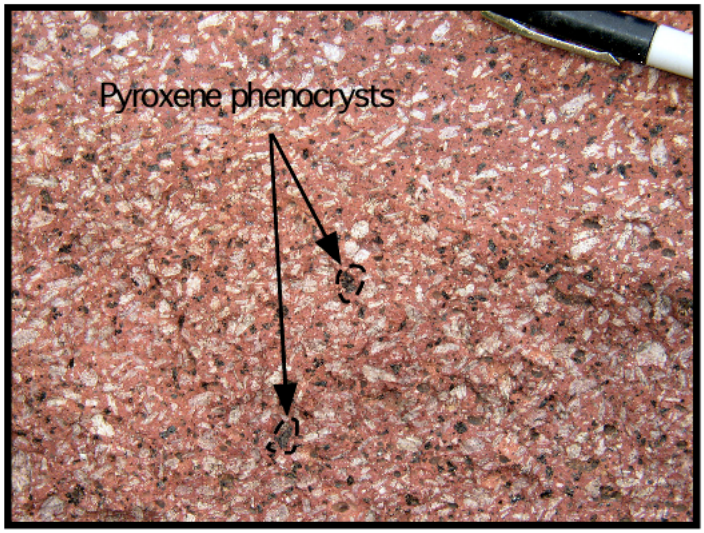

Figure12. b. Hand sample of Johnson Valley Reservoir Trachyte, used for cosmogenic ^{3}He sampling. Pyroxene (black phenocrysts) are separated from the andesite and used for the dating procedure.

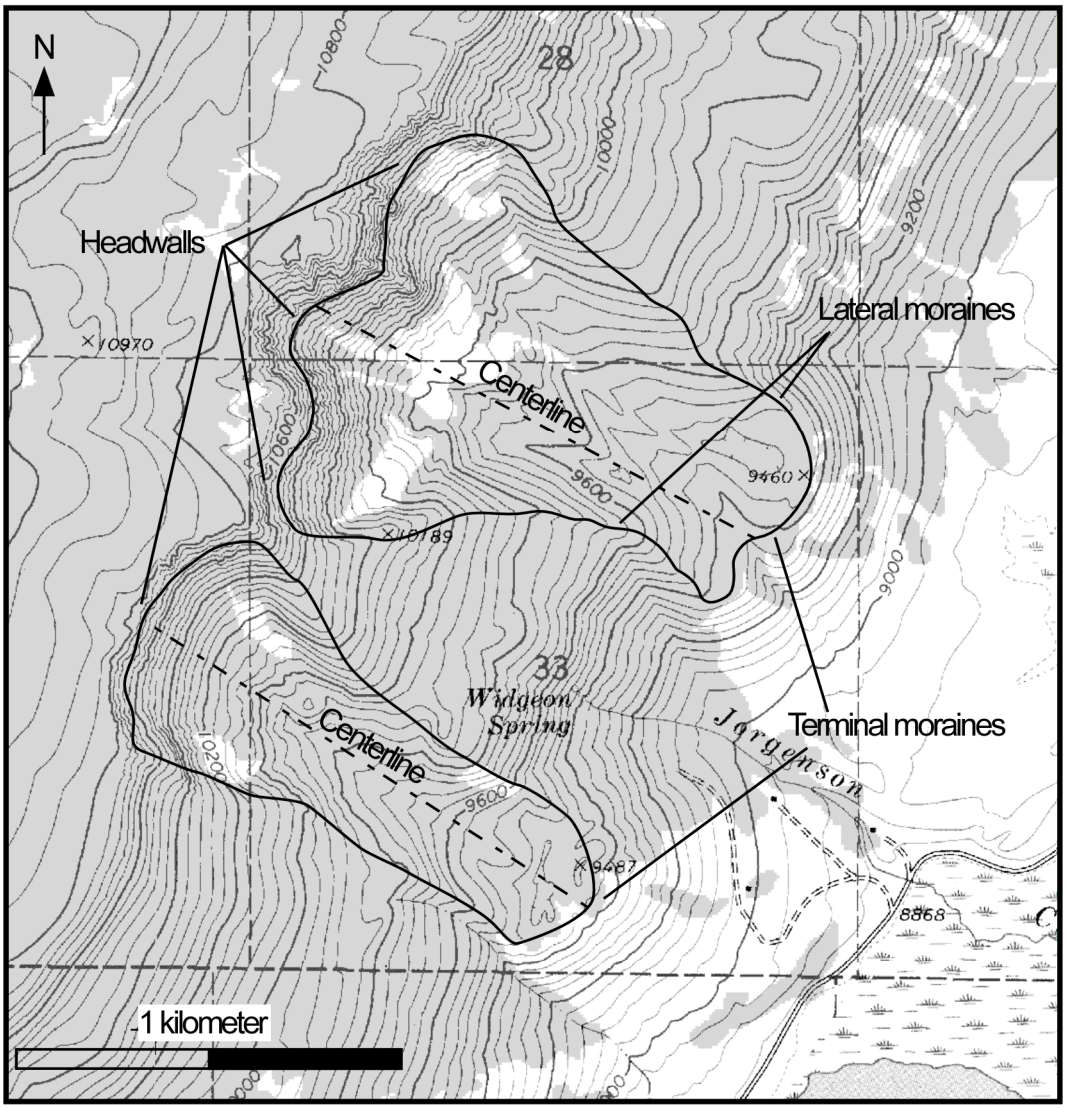

Figure 13. Schematic diagram of glacial outlines for the Jorgenson Cirques glaciers determined from topographic maps. These outlines were used as the basis of glacial reconstructions with the GlacPro Program (Locke, 2007). Glacial moraines were determined by aerial photography interpretation and location of moraine crests on topographic maps. Headwall locations were determined from valley and cirque walls. The Fish Lake and Mount Terrill 7.5-minute series quadrangle maps were used for field mapping and interpretation (U.S. Geological Survey, 2001).

The glacier areas, elevation measurements and centerline profiles used in computer modeling are taken from digitized sections of the Fish Lake and Mount Terrill topographic maps overlain by outlined paleoglaciers (Fig. 4; 2001). Hand-drawn ice-surface contours and ice flow directions from glacial reconstruction were added to outlined paleoglaciers with the Canvas X computer program.

COMPUTER MODELING

The GlacPro program, designed by William Locke of Montana State University, is a computer spreadsheet model used to reconstruct alpine paleoglaciers (Locke, 1996, 2007). I used GlacPro to develop glacial reconstructions and ice surface topography for eight Fish Lake paleoglaciers. GlacPro is a simple, transparent, spreadsheet modeling program that uses an iterative approach to glacial reconstruction. The model utilizes geomorphologic indicators of paleoglacier extent, in conjunction with known factors governing ice behavior, to reconstruct glacier morphology and ice surface contours. GlacPro best reproduces and reconstructs glaciers and creates longitudinal profiles for small, alpine glaciers with relatively simple valley or cirque geometry.

An iterative approach to glacial reconstruction is possible because ice elevation can be constrained at a glacier's terminus. The elevation difference between the scoured bedrock along a paleoglacier's centerline profile and its terminal and lateral moraines is equivalent to the former ice thickness along this same centerline, assuming that the modern moraine height is equivalent to its Pleistocene elevation and did not incur significant volume loss due to glacier recession. Beyond moraines, it is more difficult to constrain former ice surface elevation with field mapping of geomorphic features. However, ice behaves mechanically consistently, and an iterative approach to calculating

glacier hypsometry up-ice from moraines with spreadsheet models yields theoretically sound reconstruction of alpine glaciers' ice surface topography (Appendix 1**)**.

Inputs

The inputs to the GlacPro program at each step of the model are map scale; up-ice distance, which is simply the distance along a centerline profile from the glacier terminus; the step length, or distance along a centerline profile between the location of data for the current step and the previous iteration; bedrock elevation; and moraine crest elevation along a centerline path, as determined from paleoglaciers outlined on topographic maps (Fig. 4; Appendix 1). These inputs constrain ice morphology at the glacier terminus based on the concept that ice elevation does not exceed the elevation of terminal and lateral moraines at the glacier toe. If moraine crest and ice surface elevations along a well-constrained centerline path are known, then paleoglacier morphology can be determined.

Parameters

Glacial reconstruction models function because ice behaves mechanically consistently. Two factors governing ice behavior in alpine glaciers are basal shear strength and shape factor. Effective basal shear strength is a measure of the distributed force over an area at the base of a glacier that acts parallel to the basal surface (Benn and Evans, 1998). Basal shear strength is calculated at each step in the GlacPro model. For the GlacPro model I set basal shear strength at one bar based on glacier mechanical theory, or at values that match calculated ice elevations with measured moraine crest elevations at glacier termini. This approach occasionally leads to the use of modeled basal shear strengths inconsistent with glacial theory. Realistically, ice elevations do not

exceed moraine elevations at glacier termini; therefore I chose to use basal shear strengths that match ice surfaces to measured moraine elevations, despite occasional disagreement with glacial mechanical theory. For steps in the model up-ice from moraines, I set basal shear strength at one bar in keeping with glacial theory. Basal shear strength for Fish Lake paleoglaciers varies between 0.1 and one bar in GlacPro reconstructions.

Shape factor is the ratio between the hydraulic radius and the centerline ice thickness of a glacier (see Fig. 4 for centerlines used in Fish Lake paleoglacier reconstructions). The hydraulic radius is the cross-sectional area of a glacier divided by its wetted perimeter (Fig. 14). Shape factor varies between one for an infinitely wide glacier, and 0.6 for a glacier in a narrow gorge (Locke, 1996, 2007). Paleoglacier shape factor is calculated once near the terminus and once in the glacial valley. Shape factor is varied about the computed values at each step in the model. For this study, calculated shape factors often exceed or do not reach expected theoretical values between 0.6 and one. In these cases, I approximate shape factor at the nearest theoretical value. Shape factor must be included in the GlacPro program, and substituting the closest theoretical value for values that fall outside the appropriate range of 0.6 to one is the best way to determine glacier morphology given the limitations of this model. Unadjusted shape factors from Fish Lake paleoglaciers range between 0.54 and 1.45. The variance beyond theoretical values for calculated shape factor is high. This occurs because the GlacPro calculation for shape factor was designed for use with simple valley glaciers. Thus, shape factors calculated for cirque glaciers on the Fish Lake Plateau fall outside the

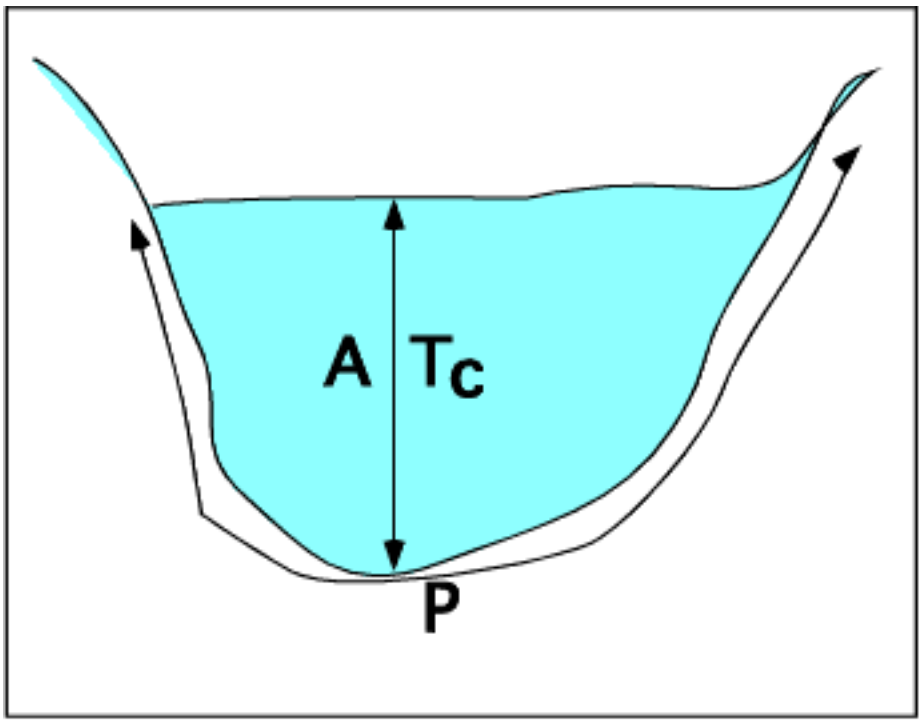

Figure 14. Generalized glacier cross-section. A. Cross-sectional area; T_c. Centerline thickness; P. wetted perimeter

expected values. However, these cirques did exist at the LGM, and approximation of the shape factor to the closest theoretical value for the purposes of the model is appropriate.

Outputs

GlacPro calculates ice thickness and ice surface elevation at each step of the model. This program uses the combination of bedrock elevation, distance along centerline paths and ice elevation estimates to create glacier longitudinal profiles (Fig. 15). Predicted ice thicknesses and elevations, as well as estimated paleoglacier geometry are not independently estimated from geomorphologic markers beyond lateral moraines. Glacial erosion up-ice from the terminus does not preserve identifiable landforms with which to constrain glacier location. The use of the GlacPro model, however, provides reasonable estimates of glacier surface elevation for the entire length of the Fish Lake paleoglaciers. The similarity between paleoglacier ice surface elevations and glacial trimlines in aerial photography of the region cannot be quantified because of heavy tree cover. However, straightforward correlation between paleo-ice surface elevations at the glacier termini indicates typical glacier behavior at terminal and lateral moraines on the Fish Lake Plateau. The mechanical consistency of ice, in conjunction with the strength of geomorphologic markers as a means to delineate ice perimeters at glacier termini, provides a strong foundation for computer modeling of glacial geometry and ice reconstruction.

Sources of error

No error is associated with the ice surface topography of Fish Lake paleoglaciers determined with computer models. Hand drawn hypsometric contours on outlined paleoglaciers are estimated from ice surface elevations determined in each step of the

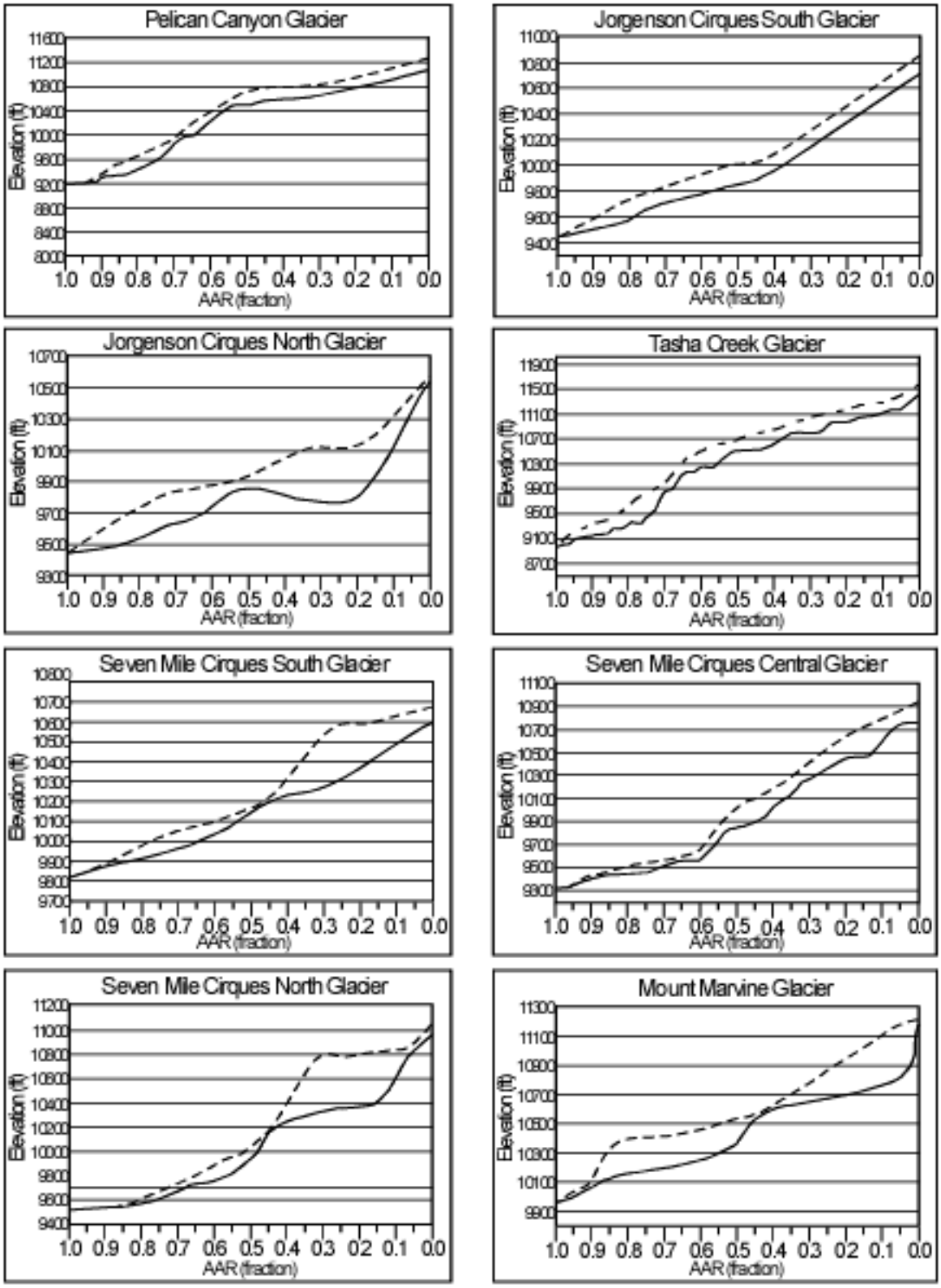

Figure 15. Bedrock and ice surface profiles for eight paleoglaciers on the Fish Lake Plateau. AAR fraction indicates the percentage of total ice area above the corresponding area. The altitude at an AAR of 0.65 + 0.05 is the predicted ELA for LGM alpine glaciers. Dashed lines denote ice elevation profiles, solid lines denote bedrock profiles.

GlacPro model. The GlacPro values are based on input of the elevations of ice marginal features identified with field mapping and aerial photography interpretation. The errors introduced by the inability to precisely define these margins are relatively insignificant. Even where uncertainties in delimiting ice margins may be large, as in former accumulation areas, the effect on glacier area is small (a few percent) because valley sides are steep and contour lines are closely spaced (Brugger and Goldstein, 1999). In up-ice glacial zones, boundaries are chosen at the upper extent of steep regions to ensure that maximum glacial volume is calculated in glacier reconstruction. There is no formal error associated with possible ice volume change resulting from differences in outlined glacier area. Volume is calculated in the GlacPro program and cannot be independently determined through field mapping and trimline identification.

There is no error associated with ice geometry or elevations calculated from glacial profiles, which were created in GlacPro (Fig. 15). Longitudinal profiles are based upon personal interpretation of glacial depositional and erosional landforms, and as such cannot be assigned quantitative error values. There is no formal error associated with the basal shear strength and shape factor values used in the GlacPro model. These values are calculated with data derived from personal interpretation of topographic features, which prevents the assignment of quantitative error to these values.

ELA RECONSTRUCTION

Ice surface contours calculated in GlacPro are hand-drawn and transferred to outlined paleoglaciers on topographic maps (Fig. 16). These contour lines are not hard and fast markers of glacier surface morphology, but rather show the most idealized glacier geometry given predicted ice surface elevations. I estimate ELAs for Pleistocene

Figure 16. Fish Lake paleoglacier reconstructions. 200 foot contour interval; contours occasionally omitted on ice surfaces. a. Pelican Canyon glacier; b. Mount Marvine glacier; c. Seven Mile Cirques; d. Jorgenson Cirques; e. Tasha Creek glacier

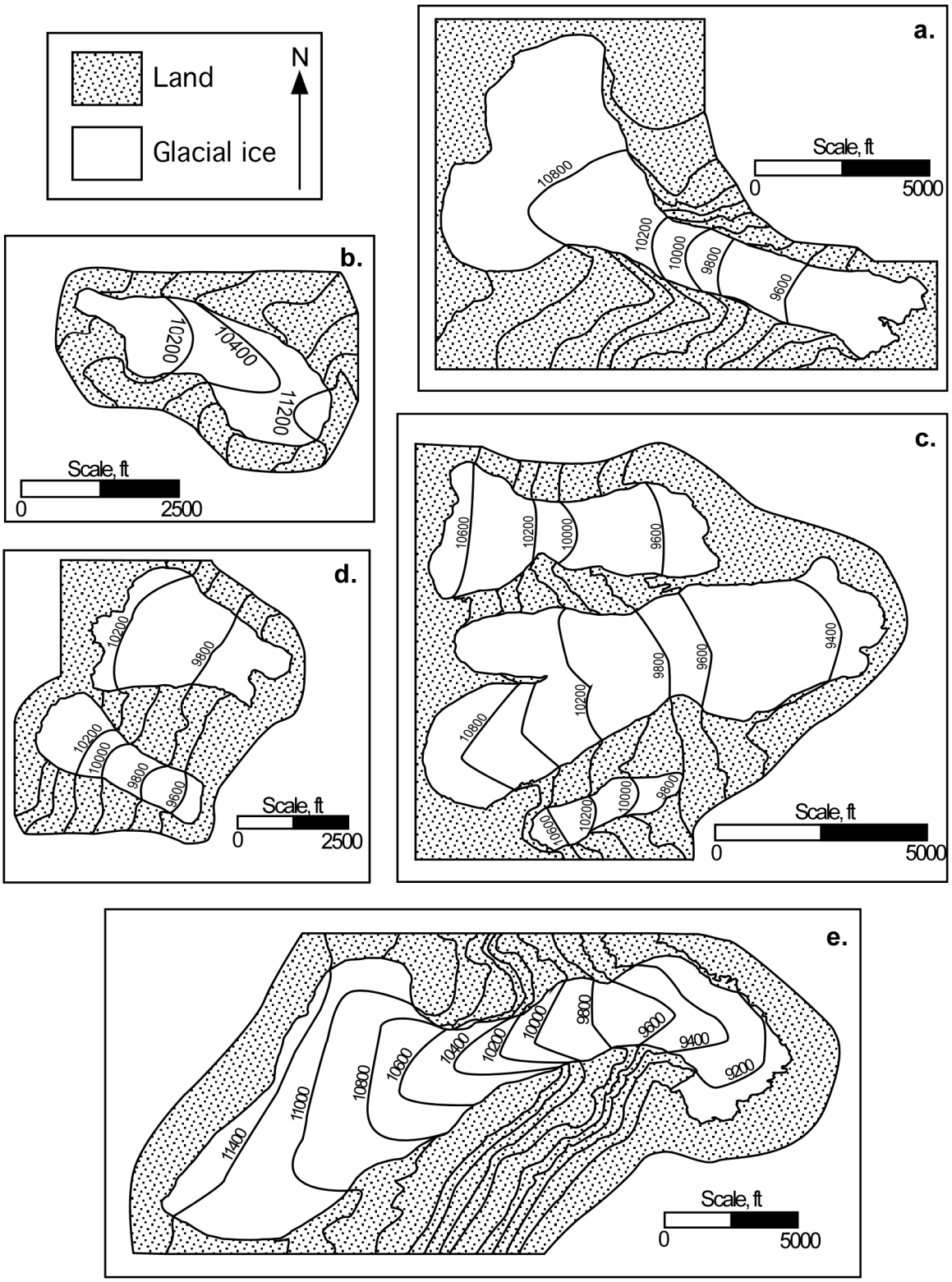

glaciers on the Fish Lake Plateau from these paleoglacier outlines and GlacPro ice surface elevation models. I calculate ELAs with a variety of approaches used in both former and modern glacial settings (c.f. Benn and Lehmkuhl, 2000; Brugger, 2006; Brugger and Goldstein, 1999; Locke, 1990; Meierding, 1982; Porter, 2001; Ramage et al., 2005). Toe to headwall altitude ratio (THAR), accumulation area ratio (AAR), cirque floor altitude and maximum altitude of lateral moraines (MALM) methods are used to approximate the ELA for each paleoglacier to within 6 m (see error analysis, c.f. Meierding, 1982; Ramage et al. 2005; Fig. 17).

MODERN ELA RECONSTRUCTION

I also use ELA reconstruction to determine the modern equilibrium-line altitude of the Fish Lake Plateau. This region is not currently glaciated; therefore I employ regression to present-day summer freezing altitudes to approximate the modern ELA. Regression to the 0º C isotherm with modern summer climate data from Loa, Utah (38º40' N, 111º64' W; 2157 m) and an assumed atmospheric lapse rate of 6º C/1 km yields a modern ELA of 4900 m (Appendix 2; National Climate Data Center, 2007).

Data from Loa, Utah is used due to the absence of consistent and reliable temperature and precipitation statistics from Fish Lake National Forest, the location of the Fish Lake Plateau. While Loa is not an alpine setting, the regression from these measurements remains an acceptable approximation for the mean summer 0º C isotherm, and the predicted modern ELA. If anything, this regression underestimates the modern July 0º C isotherm in south-central Utah. I use summer data rather than July climate records alone in regression to the 0º C isotherm. Full NOAA climate data for this region spans only 30 years; therefore the use of values from June, July and August provides the

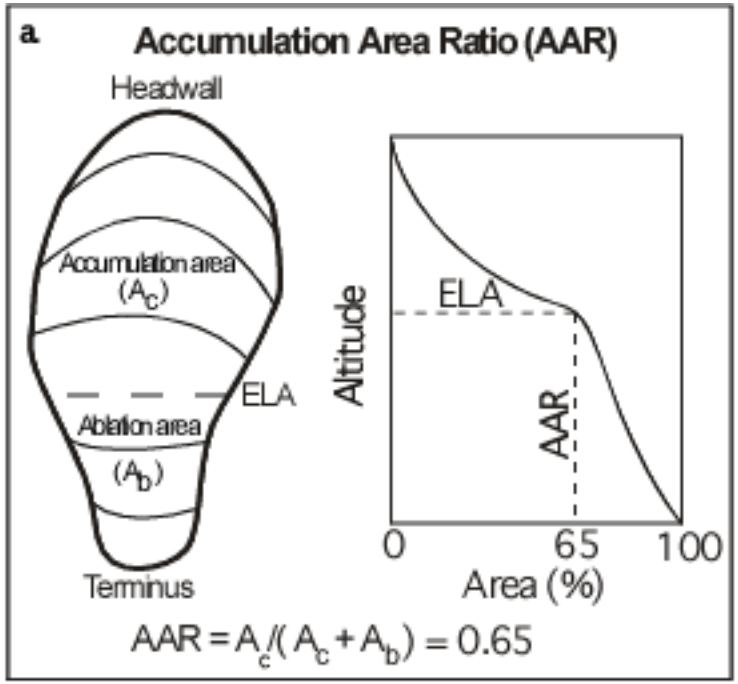

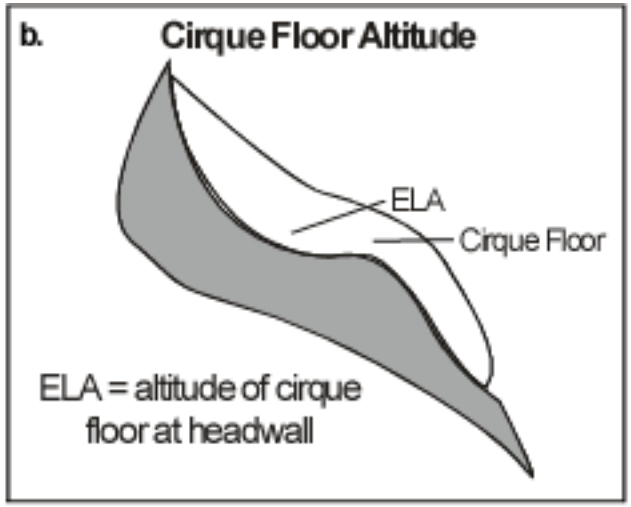

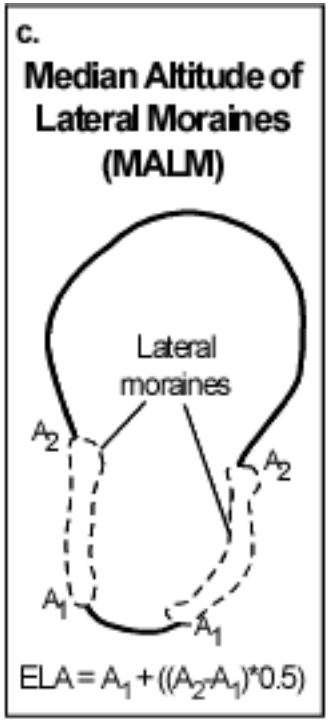

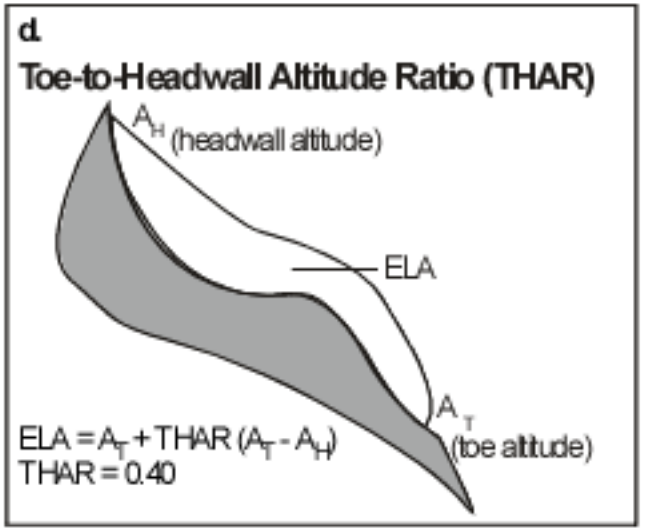

Figure 17. Schematic diagram for ELA derivations after Porter (2001). a. ELA derivation from AAR (0.65), the area of the glacier is plotted along the GlacPro longitudinal profile, the ELA is the altitude where accumulation area constitutes 65% of total glacier area; b. ELA derivation from cirque floor altitude; c. ELA derivation from median altitude of lateral moraines; d. ELA derivation from toe-to-headwall altitude ratio, the empirically derived THAR is set at 0.40.

most comprehensive climate dataset for south-central Utah. However, June temperatures are consistently cooler than those in July and August, which may lower the overall average summer temperature of Loa, decreasing the calculated 0º C isotherm estimated from linear regression. Nevertheless, a present-day ELA of 4900 m is employed in this analysis, and corresponds to estimates from previous studies (e.g. Mulvey, 1985).

There is no error associated with modern ELA estimates. This theoretical value is based upon known climate data and an assumed atmospheric lapse rate. The lapse rate comes from values used in other studies of late Pleistocene glaciation in the western United States (c.f. Galloway, 1970; Porter, 1977; Laabs, 2004). The use of alternate atmospheric lapse rates and modern climate data will yield significantly different late Pleistocene ELAs for the Fish Lake Plateau. However, the values used were chosen for their proximity to the study area (modern climate data) and their agreement with previous studies (atmospheric lapse rate). The 4900 m modern ELA estimate yields Pleistocene ELAs and summer temperature depressions consistent with other studies from the region and is acceptable for the purposes of this study.

PLEISTOCENE ELA RECONSTRUCTION

Toe to headwall altitude ratio (THAR)

The THAR relies on the assumption that ELAs for modern glaciers fall approximately midway between the altitudes of glacier headwalls versus glacier termini (Ramage et al., 2005). THAR values between 0.35 and 0.45 are commonly used for paleoglacier reconstruction (Meierding, 1982). For this study I use a THAR of 0.40 to calculate LGM ELAs. This assumption yields late Pleistocene ELAs between approximately 3000 and 3200 m (Appendix 2).

Accumulation area ratio (AAR)

The AAR method comes from an empirically derived ratio between accumulation zone area and total glacier area, which falls between 0.5 and 0.8 (Ramage et al., 2005). An AAR of 0.65 is used for the Fish Lake paleoglaciers. This ratio indicates that accumulation area occupies 65% of total glacier area. Using the AAR method, Fish Lake ELAs fall between 3000 and 3200 m (Appendix 2). ELA values derived from AAR calculations with an AAR of 0.65 are assigned an error of $\pm$ 0.05. This corresponds to a difference in area of roughly $\pm$ 5% in total glacier area based upon the work of Leonard (1984).

Cirque floor altitude

Cirque floor altitudes provide a rough estimate of equilibrium-line altitude for small alpine glaciers (Meierding, 1982). This method is applied to the Jorgenson Cirques, Mount Marvine and the Seven Mile Cirques. The cirque floor altitude method is applicable to ELA calculation for the Mount Marvine paleoglacier because of its cirque-like geometry. Estimated cirque floor altitude ELAs are between 3050 and 3230 m (Appendix 2).

Maximum altitude of lateral moraines (MALM)

Elevation at the upper limit of lateral moraines provides a first approximation of late Pleistocene ELAs for the Fish Lake region. This method gives a minimum ELA because moraines only form in the ablation zone of a glacier (Ramage et al., 2005). MALM ELAs for the Fish Lake Plateau fall between roughly 3000 and 3100 m (Appendix 2).

ELA values from MALM, THAR and cirque headwall altitudes are set at ± 6 m. These ELA determinations depend on identification of glacial geomorphic features in the field and their transference onto 1:24,000 USGS topographic maps with 40 foot (approximately 12 m) contour intervals. In general, the elevations of these features can be identified to within ± 6 m.

RESULTS

Comparison between Pleistocene and modern ELAs on the Fish Lake Plateau indicates depressions of 1650 to 1950 m below the 4900 m modern ELA (Appendix 2). Four separate ELA determination methods yield late Pleistocene ELAs between 2950 and 3250 m. Lowered Fish Lake ELAs during the late Pleistocene correspond to an LGM summer temperature depression of 10º to 12º C, assuming a steady-state atmospheric lapse rate of 6º C/1 km.

Pelican Canyon was a 4 km^2 southeast-facing glacier with late Pleistocene ELAs between 3043 and 3109 m. Jorgenson Cirques South (0.5 km^2) faced southeast with LGM ELAs of 2987 to 3108 m. Jorgenson Cirques North (0.9 km^2) faced southeast with ELAs between 3002 and 3048 m. The Tasha Creek paleoglacier (13.4 km^2) faced east. Tasha Creek ELAs range from 3028 to 3155 m. The Seven Mile Cirques faced northeast. The southernmost cirque was 0.3 km^2 with ELAs between 3072 and 3170 m. The central cirque was 3.3 km^2 with ELAs between 2926 and 3231. The northernmost cirque was 1.3 km^2 with ELAs between 2987 and 3170 m. The Mount Marvine paleoglacier (0.5 km^2) faced northwest with ELAs between 3109 and 3187 m (Appendix 2).

DISCUSSION AND CONCLUSIONS

While temperature has varied over the past 21 ka, moisture levels and hydrologic sources for the Rocky Mountains have not changed significantly since the LGM. In a study of Pleistocene ELAs and modern snowline in the San Juan Mountains, CO, Leonard (1984) notes a correlation between the west-to-east rise in both paleo-ELAs and modern snowline. The author argues that the similarity in pattern and gradient of late Pleistocene ELAs and modern snow levels in the San Juan Mountains indicates no major change in circulation between the LGM and the present. If no circulation change has occurred, then accumulation season wind patterns and moisture sources must have remained consistent between the late Pleistocene and the present (Leonard, 1984). This similarity in moisture sources since the LGM suggests that Pleistocene ELA depressions on the Fish Lake Plateau were primarily due to changes in temperature.

Modeling indicates alpine glaciers in the American West exhibit differences in their sensitivities to climate forcing. However, changes in temperature tend to dominate over changes in precipitation (Hostetler and Clark, 1997). A cold, dry climate suggests that summer temperature depressions rather than winter precipitation increases accounted for the majority of enhanced LGM snow accumulation and glaciation on the Fish Lake Plateau. Glacial environments require year-round snow pack. This condition is met when winter snowfall exceeds summer loss, when low summer temperatures inhibit melting, or under a combination of low-temperature, high-precipitation conditions. Thus, Pleistocene Utah required decreased summer temperatures to maintain alpine glaciers under a precipitation regime similar to, or drier than modern levels.

While summer temperature depression estimates for Fish Lake are on par with previous studies for Pleistocene glaciations in Utah, they exceed many estimates from studies of the Rocky Mountains (Mulvey, 1985; Anderson et al., 2000; Betancourt et al., 2003; see Table 1). The increased magnitude of LGM temperature depression in the High Plateaus compared to other regions of the western United States may be due to a local increased moisture source from glacial Lake Bonneville, which was at Stansbury shore levels during the LGM (Fig. 2; Munroe et al., 2006). Munroe et al. (2006) suggest that correspondence between the maximum extent of Pleistocene glaciers and Lake Bonneville shorelines indicates a synchronous reaction to the northward migration of the polar jet stream due to the collapse of the Laurentide Ice Sheet.

At Stansbury levels, the 47,800 km^2 Lake Bonneville provided winter season precipitation to the Bonneville Basin. This Lake Bonneville moisture source added to precipitation from Pacific storm tracks traveling from east to west. The increased moisture levels effectively lowered the regional ELA for glacier populations throughout the Bonneville Basin (Hostetler et al., 1994). The geographic extent of this "lake effect" is unknown; although, increased winter precipitation levels may have extended to the High Plateaus of Utah. Moisture enhancement on the Fish Lake Plateau due to changes in circulation as a result of the transgression of Lake Bonneville shorelines may help to explain the relatively large ELA depressions recorded at the LGM.

In this study calculated ELA depressions indicate maximum ablation season temperature depressions, assuming that decreased ELAs were due solely to changes in temperature, rather than a combination of changes in both temperature and precipitation. This is a reasonable assumption given previous modeling of climatic controls on western

Location	State	Temperature Depression (*C)	Reference
Bear River Range	UT	14	Mulvey, 1985
Wasatch Range	UT	14	Mulvey, 1985
Bonneville Basin	UT	13	Gates, 1976
Lake Bonneville and Lake Lahontan	UT and NV	11 to 13	Hostetler et al., 1994
Northern New Mexico	NM	9	Leopold, 1951
San Juan Range	CO	10 to 13	Leonard, 1989
Sawatch Range	CO	7 to 9	Brugger & Goldstein,
Sawatch Range	CO	7 to 8.5	Brugger, 2006
Front Range	CO	10 to 13	Leonard, 1989
Southwestern U.S.	——	10 to 11	Galloway, 1970
Wyoming Basin	WY	14	Mears, 1981
Western Montana	MT	10	Locke, 1990
Cascade Range	WA	5.5	Porter, 1977
Western U.S.	——	8 to 18	Hostetler and Clark, 1997
Global Sea Surfaces	Global Oceans	10	COHMAP Members, 1988

Table 1. Late Pleistocene glacial population locations and estimated summer temperature depressions from studies of the western United States. Modified from Meierding (1982) and Mulvey (1985).

U.S. glaciers, which suggests summer temperatures are the driving force behind alpine glacier ELAs (e.g. Hostetler and Clark, 1997).

However, it is impossible to definitively attribute Pleistocene ELA depressions to a specific temperature-precipitation regime. These conditions evolve coevally and their interactions drive the Earth's climate system. A measured ELA depression of 1500 m may indicate a summer temperature depression of 9º C, or a precipitation increase of 250%, however, in all likelihood the difference between modern and paleo-ELAs is the result of changes in both of these facets of climate.

The relative contribution of temperature versus precipitation on equilibrium-line altitude cannot be determined for Fish Lake paleoglaciers because there are no definitive values for LGM temperature or precipitation in the region. However, given modern alpine glaciers' sensitivity to summer season temperature, I choose to focus on the predicted magnitude of LGM temperature depression. To do this, I assume precipitation conditions in the Intermountain West have not varied significantly over the past 21 ka. Although moisture enhancement from Lake Bonneville likely played some role in the development of LGM paleoglaciers on the Fish Lake Plateau, this precipitation effect was probably much weaker than that of temperature on late Pleistocene ice growth.

In addition to the possible enhancement effect of Lake Bonneville, large predicted LGM summer temperature depressions at Fish Lake may be overestimated due to the limited resolution of this study. Continental paleoclimate records vary due to the proxy chosen and methods employed for a particular study. The proxy selected determines the sensitivity and range of the analyzed paleoclimate signal. Continental paleoclimate proxies include pollen and fossil records, as well as glacier ELAs. The temperature

depression estimates for the Fish Lake Plateau are consistently higher than those from western U.S. studies employing other paleoclimate signals (e.g. Anderson et al., 2000; Betancourt et al., 2001; Kaufman, 2003). In contrast to paleoclimate studies employing proxies correlated across a large region, such as pollen records, the number of Pleistocene paleoglaciers on the Fish Lake Plateau inherently limits this study. There are only eight identifiable paleoglaciers in the Fish Lake region, therefore it is impossible to do trend-surface contouring of topography and paleoglacier location across a sizeable area (c.f. Meierding, 1982). The lack of identified regional trend surfaces prevents differentiation between broad trends in glacier location and style versus trends due to local anomalies in topography or circulation. Associations between Pleistocene alpine glacier populations located more than 500 km away from the Plateau are unreliable given the extent of regional trends in glaciation (Letreguilly and Reynaud, 1989). The inability to compare Fish Lake paleoglaciers with other alpine glacier populations in the Rocky Mountains limits the applicability of this study to a broader context.

Due to the heavy influence of local environment on small alpine glaciers, the hypsometry of LGM paleoglaciers on the Fish Lake Plateau was probably controlled by local topography. Thus, anomalies due to local topography, as well as general trends in LGM climate and circulation caused the calculated ELA depressions and climate patterns from this study. The application of these summer temperature depression estimates to areas beyond the High Plateaus is difficult due to the integral role of microclimate and regional characteristics in determining alpine glacier geometry.

However, within-population comparisons can be made for the Fish Lake paleoglaciers. Low AAR-type ELAs for the Seven Mile Cirques suggest aspect played a

significant role in determining equilibrium-line altitude for LGM glaciers on the Fish Lake Plateau. The Seven Mile Cirques trend northeast, and as a result receive reduced insolation levels in comparison to the southeast-facing Jorgenson Cirques, which have relatively high ELAs.

ELA differences between Fish Lake paleoglaciers also indicate that Mytoge Mountain, and Mount Marvine provided significant shading for Pelican Canyon, the Jorgenson Cirques, and the Seven Mile Cirques. Shading allowed sizeable alpine glaciers to develop on east and southeast-facing slopes, despite relatively high insolation levels. Calculated AAR-type ELAs from Pelican Canyon, the Jorgenson Cirques, and the Seven Mile Cirques, which are shaded by Mytoge Mountain and Mount Marvine, are lower than those calculated for the northwest-trending Mount Marvine paleoglacier. The lack of shading for Mount Marvine probably prevented the development of a large ice mass, despite its glacially favorable northwest aspect.

The largest LGM glacier in the region, Tasha Creek paleoglacier, has the highest AAR-type ELA on the Fish Lake Plateau. This situation illustrates the combined effect of aspect and shading on glacier development. Tasha Creek faces east, and thus received mid-range insolation levels at the LGM. Additionally, part of the Tasha Creek paleoglacier was shaded by Mytoge Mountain, allowing increased glacier development in the shaded region. These conditions indicate that Tasha Creek would have had a low LGM ELA. However, this is mitigated by the icecap morphology of the paleoglacier. The Tasha Creek icecap that existed on the Fish Lake Hightop was not shaded and would have received maximum insolation levels, effectively raising the ELA for the entire

glacier, despite shading in the glacier valley. These conditions help to explain the high ELA of the large Tasha Creek paleoglacier.

I exclusively compare AAR-type ELAs for within-population analysis of LGM glaciers from the Fish Lake Plateau. The accumulation-area ratio method is the most rigorous method used to calculate ELAs for alpine glaciers. In contrast to the THAR, MALM and cirque floor altitude methods, the AAR method takes into account glacier hypsometry and geometry in the ELA calculation. The THAR, MALM and cirque floor altitude methods are useful as first-order approximations of equilibrium-line altitude, however, they do not provide adequate sensitivity to local topography for comparison within a region as limited as the Fish Lake Plateau.

Continental climate reconstruction is difficult for many reasons. Analyses are limited by study area, the proxies available for study, and signal resolution. However, alpine glacial reconstruction is a valuable tool in the first-order estimation of climatic conditions in the late Pleistocene-era western United States. The unique features of glacial depositional and erosional landforms ensure their field recognition, and the identification of paleoglacier location with topographic map and aerial photography interpretation. Additionally, the mechanical consistency of ice guarantees straightforward and relatively well-constrained glacier reconstruction with an iterative computer spreadsheet model. Rigorous climate reconstruction with known constraints on temperature and precipitation values is not possible through comparison of modern and paleo-ELAs because of the duality between temperature and precipitation as components of the climate system. However, Pleistocene glacier and ELA reconstructions provide general estimates for both local and regional climate change since the LGM. This

approach is particularly valuable in the Intermountain West where evidence of paleoglaciation is abundant, and the mechanics of alpine glaciation are well understood. This study of LGM glaciers on the Fish Lake Plateau provides an initial model for late Pleistocene climate in south-central Utah. Comparison with studies of LGM glaciation in other areas of the western United States shows similar, although slightly increased summer temperature depressions on the Fish Lake Plateau. Regardless of the variance in magnitude between Fish Lake ELA depressions relative to previous studies, however, it is clear that the significant difference between modern and late Pleistocene equilibrium-line altitudes is due at least in part to lowered summer season temperatures under a cool, dry glacial climate in the western United States at the Last Glacial Maximum.

ACKNOWLEDGEMENTS

I would first and foremost like to thank my advisors Chuck Bailey at the College of William & Mary, Dave Marchetti at Colgate University, and Mary Savina at Carleton College for their help on this project. They have been invaluable resources and have provided countless hours of guidance throughout this process. I would also like to thank Sarah Titus for her helpful suggestions on this paper. This project was made possible through the Fish Lake Research Experience for Undergraduates program at the College of William & Mary with funding from the National Science Foundation. I would like to thank the entire Carleton College Geology Department for their financial support, general guidance and enthusiasm; and my fellow geology majors, specifically the fantastic class of 2007.

REFERENCES

Anderson, R.S., Betancourt, J.L., Mead, J.I., Hevly, R.H., and Adam, D.P., 2000, Middle-and-late Wisconsin paleobotanic and paleoclimatic records from the southern Colorado Plateau, USA: Palaeogeography, Palaeoclimatology, Palaeoecology, v. 155, p. 31-57.

Adams, J., Oak Ridge National Laboratory: North America during the last 150,000 years, http://www.esd.ornl.gov/projects/qen/nercNORTHAMERICA.html, accessed March 5, 2007.

Bailey, C. M., Harris, M. S., and Marchetti, D. W., 2007, Geologic overview of the Fish Lake Plateau, Utah; unpublished manuscript: Williamsburg, College of William & Mary, 13 p.

Benn, D. I., and Evans, D. J. A., 1998, Glaciers & glaciation: Wiley, New York 734 p.

Benn, D. I., and Lehmkuhl, F., 2000, Mass balance and equilibrium-line altitudes of glaciers in high-mountain environments: Quaternary International, v. 65-66, p. 15-29.

Betancourt, J. L., Aasen-Rylander, K., Penalba, C., and McVicker, J. L., 2001, Late Quaternary vegetation history of Rough Canyon, south-central New Mexico, USA: Palaeogeography, Palaeoclimatology, Palaeoecology, v. 165, p. 71-95.

Brugger, K.A., 2006, Late Pleistocene climate inferred from the reconstruction of the Taylor River glacier complex, southern Sawatch Range, Colorado: Geomorphology, v. 75, p. 318-329.

Brugger, K.A., and Goldstein, B.S., 1999, Paleoglacier reconstruction and late Pleistocene equilibrium-line altitudes, southern Sawatch Range, Colorado: Geological Society of America Special Papers, v. 337, p. 103-112.

Cerling, C. E., and Craig, H., 1994, Geomorphology and in-situ cosmogenic isotopes: Annual Review of Earth and Planetary Science, v. 22, p. 273-317.

Chadwick, O.A., Hall, R.D., Phillips, F.M., 1997, Chronology of Pleistocene glacial advances in the central Rocky Mountains: GSA Bulletin, v. 109, p. 1443-1452.

COHMAP Members, 1988, Climatic changes of the last 18,000 years: observations and model simulations: Science, v. 241, p. 1043-1052.

Dickson, T.A., Fairchild, J.M., Coor, J.L., Bailey, C.M., and Marchetti, D.W., 2006, Grabens of the Fish Lake Plateau, High Plateaus, Utah: Geological Society of

America Abstracts with Programs, v. 38, no. 6, p. 11.

Galloway, R., 1970, The full-glacial climate in the southwestern United States: Annals of the Association of American Geographers, v. 60, p. 245-256.

Gates, W.L., 1976, Modeling the ice age climate: Science, v. 191, p. 1138-1144.

Hardy, C.T., and Muessig, S., 1952, Glaciation and drainage changes in the Fish Lake Plateau, Utah: GSA Bulletin, v. 63, p. 1109-1116.

Hooke, R. L., 2005, Principles of Glacier Mechanics: Cambridge, Cambridge University Press, 429 p.

Hostetler, S. W., and Clark, P. U., 1997, Climatic controls of western US glaciers at the last glacial maximum: Quaternary Science Reviews, v. 16, p. 505-511.

Hostetler, S. W., Giorgi, F., Bates, G. T., and Bartlein, P. J., 1994, Lake-atmosphere feedbacks associated with paleolakes Bonneville and Lahontan: Science, v. 263, p. 665-668.

Kaufman, D.S., 2003, Amino acid paleothermometry of Quaternary ostracodes from the Bonneville Basin, Utah: Quaternary Science Reviews, v. 22, p. 899-914.

Laabs, B. J. C., 2004, Late quaternary glacial and paleoclimate history of the southern Uinta Mountains, Utah [Ph.D. thesis]: Madison, University of Wisconsin, 163 p.

Leonard, E. M., 1984, Late Pleistocene equilibrium-line altitudes and modern snow accumulation patterns, San-Juan Mountains, Colorado, USA: Arctic and Alpine Research, v. 16, p. 65-76.

-, 1989, Climatic change in the Colorado Rocky Mountains: estimates based on modern climate at late Pleistocene equilibrium lines: Arctic and Alpine Research, v. 21, p. 245-255.

Leopold, L.B., 1951, Pleistocene climate in New Mexico: The American Journal of Science, v. 249, p. 152-168.

Letreguilly, A., and Reynaud, L., 1989, Spatial patterns of mass-balance fluctuations of North American glaciers: Journal of Glaciology, v. 35, p. 163-168.

Licciardi, J. M., Clark, P. U., Brook, E. J., Elmore, D., and Sharma, P., 2004, Variable responses of western US glaciers during the last deglaciation: Geology, v. 32, p. 81-84.

Locke, W. W., 1989, Present climate and glaciation of western Montana, USA: Arctic and Alpine Research, v. 21, p. 234-244.

-, 1990, Late Pleistocene glaciers and the climate of Western Montana, USA: Arctic and

Alpine Research, v. 22, p. 1-13.
-, 1996, Teaching geomorphology through spreadsheet modelling: Geomorphology, v. 16, p. 251-258.
-, GlacPro computer spreadsheet model, http://www.homepage.montana.edu/~ueswl/spreadsheet.html, accessed March 5, 2007.

Mears, B. Jr., 1981, Periglacial wedges and the late Pleistocene environment of Wyoming's intermountain basins: Quaternary Research: vol. 15, p. 171-198.

Meierding, T. C., 1982, Late Pleistocene glacial equilibrium-line altitudes in the Colorado Front Range: a comparison of methods: Quaternary Research, v. 18, p. 289-310.

Mickelson, D. M., Clayton, L., Fullerton, D. S., and Borns, H. W. J., 1983, The late Wisconsin glacial record of the Laurentide Ice Sheet in the United States, *in* Porter, S. C., ed., Late-Quaternary environments of the United States: Minneapolis, University of Minnesota Press, p. 3-37.

Molnia, B.F., Alaskan Glaciers: USGS website, http://www.usgs.gov/features/glaciers2.html, accessed 28 February 2007.

Mulvey, W. E., 1985, Reconstruction and interpretation of late Pleistocene equilibrium-line altitudes in the Lake Bonneville region [Master's of Science thesis]: Salt Lake City, University of Utah, 65 p.

Munroe, J. S., Laabs, B. J. C., Shakun, J. D., Singer, B. S., Mickelson, D. M., Refsnider, K. A., and Caffee, M. W., 2006, Latest Pleistocene advance of alpine glaciers in the southwestern Uinta Mountains, Utah, USA: Evidence for the influence of local moisture sources: Geology, v. 34, p. 841-844.

Murray, D. R., and Locke, W. W., 1989, Dynamics of the Late Pleistocene Big Timber glacier, Crazy Mountains, Montana, USA: Journal of Glaciology, v. 35, p. 183-190.

National Climate Data Center, National Oceanic & Atmospheric Administration, U.S. Department of Commerce, accessed March 5, 2007, http://www.ncdc.noaa.gov/DLYNRMS/dnrm?coopid=425148: Climatography of the United States NO. 84, 1971-2000; Loa, Utah, station 425148; United States Climate Normals, 1971-2000.

Porter, S. C., 1975, Equilibrium-line altitudes of late Quaternary glaciers in south Alps, New Zealand: Quaternary Research, v. 5, no. 1, p. 27-47.
-, 1977, Present and past glaciation threshold in the Cascade Range, Washington, U.S.A.: Topographic and climatic controls, and paleoclimatic implications: Journal of Glaciology, v. 18, p. 101-116.

-, 1986, Pattern and forcing of Northern Hemisphere glacier variations during the last millennium: Quaternary Research, v. 26, p. 27-48.
-, 2001, Snowline depression in the tropics during the last glaciation: Quaternary Science Reviews, v. 20, p. 1067-1091.

Porter, S. C., Pierce, K. L., and Hamilton, T. D., 1983, Late Wisconsin mountain glaciation in the western United States, *in* Porter, S. C., ed., Late-Quaternary Environments of the United States: Minneapolis, University of Minnesota Press, p. 71-111.

Ramage, J. M., Smith, J. A., Rodell, D. T., and Seltzert, G. O., 2005, Comparing reconstructed Pleistocene equilibrium-line altitudes in the tropical Andes of central Peru: Journal of Quaternary Science, v. 20, p. 777-788.

Thackray, G. D., 1999, Extensive early and middle Wisconsin glaciation on the western Olympic Peninsula, Washington, and the variability of Pacific moisture delivery to the northwestern United States: Quaternary Research, v. 55, p. 257-265.

Thackray, G. D., Lundeen, K. A., and Borgert, J. A., 2004, Latest Pleistocene alpine glacier advances in the Sawtooth Mountains, Idaho, USA: reflections of midlatitude moisture transport at the close of the last glaciation: Geology, v. 32, p. 225-228.

Thompson, R. S., Whitlock, C., Bartlein, P. J., Harrison, S. P., and Spaulding, W. G., 1993, Climatic changes in the western United States since 18,000 yr B.P., *in* Wright, H. E. J., Kutzbach, J. E., Webb, T. I., Ruddiman, W. F., Street-Perrott, F. A., and Bartlein, P. J., eds., Global climates since the last glacial maximum: Minneapolis, University of Minnesota Press, p. 468-513.

Titayeva, N. A., 1994, Nuclear geochemistry, advances in science and technology: Moscow, Mir Publishers, 296 p.

U.S. Department of Agriculture, 2001, Aerial Photography, Fish Lake National Forest: F4080, region 04, color negative, 100% cover, project area 614083, line index 2, 1:15,480 scale; http://www.fsa.usda.gov/Internet/FSA_File/fstxta.txt, accessed March 6, 2007.

U.S. Geological Survey, 2001, Fish Lake Quadrangle, Utah, 7.5-minute series topographic map, 38111-E6-TF-024, NIMA 3661 II SW-series V897, scale 1:24,000, 2 sheet; produced by the United States Geological Survey 1968, revision by USDA Forest Service 2001, planimetry derived from imagery taken 1997, Public Land Survey System.

U.S. Geological Survey, 2001, Mount Terrill Quadrangle, Utah, Sevier County, 7.5-minute series topographic map, 38111-F6-TF-024, NIMA 3661 II NW-series

V897, scale 1:24,000, 1 sheet; produced by the United States Geological Survey 1968, revision by USDA Forest Service 2001, planimetry derived from imagery taken 1997, Public Land Survey System.

Van der Veen, C. J., 1999, Fundamentals of glacier dynamics: Rotterdam, A.A. Balkema, 462 p.

Walker, M., 2005, Quaternary dating methods: West Sussex, John Wiley & Sons Ltd, 286 p.

Weaver, W. J. IV, Marchetti, D. W., Stoll, D. K., Harris, M. S., and Bailey, C. M., 2006, ^{3}He exposure ages for glacial deposits, Fish Lake Plateau, Utah: Geological Society of America Abstracts with Programs, v. 38, no. 6, p. 30.

Webber, C. E., 2003, Structural and fluvial history of the Fish Lake basin, High Plateaus, central Utah [undergraduate thesis]: Williamsburg, College of William & Mary.

Zwick, T. T., 1980, A comparison between the modern and composite Pleistocene snow-lines, Absaroka and Beartooth mountains, Montana-Wyoming, U.S.A.: The Journal of Glaciology, v. 25, no. 92, p. 347-352.

UPICE DIST. (ft)	BEDROCK ELEVATION (ft)	SHAPE FACT.	BASAL SHEAR (bar)	Step Length (ft)	Change (ft)	Calculated Elevation (ft)	Centerline Thickness (ft)	MORAINE CREST (ft)	Ice Thickness (ft)
0	9200					9200	0	9200	0
483	9220					9230	10	9230	10
966	9240					9300	60	9300	60
1449	9320	1	0.4	483	71	9371	51	9420	100
1932	9340	0.9	0.5	483	116	9487	147	9480	140
2415	9350	0.9	0.65	483	52	9539	189	9500	150
2898	9370	0.9	0.7	483	44	9583	213	9560	190
3381	9420	0.75	0.8	483	53	9637	217	9650	230
3864	9480	0.75	1	483	66	9702	222	9760	280
4347	9560	0.75	1	483	64	9766	206	9840	280
4830	9620	0.8	1	483	65	9831	211		
5313	9730	0.8	1	483	63	9894	164		
5796	9880	0.8	1	483	81	9975	95		
6279	9980	0.8	1	483	140	10115	135		
6762	9980	0.83	1	483	95	10210	230		
7245	10090	0.8	1	483	58	10268	178		
7728	10180	0.8	1	483	75	10343	163		
8211	10270	0.8	1	483	82	10425	155		
8694	10400	0.8	1	483	86	10511	111		
9177	10490	0.8	1	483	120	10631	141		
9660	10500	0.8	1	483	94	10726	226		
10143	10580	0.8	1	483	59	10785	205		
10626	10670	0.8	1	483	65	10850	180		
11109	10880	0.8	1	483	74	10924	44		
11592	10970	0.8	1	483	303	11227	257		
11963	11080	0.8	1	371	40	11267	187		

Appendix 1. GlacPro spreadsheet model for Pelican Canyon Glacier, Fish Lake Plateau, Utah. Inputs to the program are upice distance, bedrock elevation, shape factor, basal shear strength, step length, and moraine crest elevation. Change, calculated elevation, centerline thickness, and ice thickness are the model outputs.

Glacier	Aspect	Area (km^2)	Minimum Elevation (m)	Maximum Elevation (m)	ELA_{AAR} (m)	ELA Depression (m)	ΔT (^oC)	ELA_{THAR} ± 6 (m)	ELA Depression (m)	ΔT (^oC)	ELA Cirque Floor Altitude ± 6 (m)	ELA Depression (m)	ΔT (^oC)	ELA_{MALM} ± 6 (m)	ELA Depression (m)	ΔT (^oC)
Pelican Canyon	SE	4.0	9200	11160	3109 ± 61	1791	11	3043	1857	11	N/A	N/A	N/A	3060	1840	11
Jorgenson Cirques South	SE	0.5	9480	10720	3108 ± 30	1882	11	3036	1864	11	3048	1852	11	2987	1913	11
Jorgenson Cirques North	SE	0.9	9440	10520	3002 ± 15	1898	11	3009	1891	11	3048	1852	11	3011	1889	11
Tasha Creek	E	13.4	8960	11400	3155 ± 107	1745	10	3028	1872	11	N/A	N/A	N/A	3048	1852	11
Sevenmile Cirques South	NE	0.3	9840	10680	3078 ± 15	1822	11	3102	1798	11	3170	1730	10	3072	1828	11
Sevenmile Cirques Central	NE	3.3	9320	10800	2926 ± 15	1974	12	3021	1879	11	3231	1669	10	3085	1815	11
Sevenmile Cirques North	NE	1.3	9520	10800	2987 ± 30	1913	11	3058	1842	11	3170	1730	10	3036	1864	11
Mount Marvine	NW	0.5	9960	11200	3185 ± 15	1715	10	3187	1713	10	N/A	N/A	N/A	3109	1791	11

Appendix 2. Aspect and equilibrium-line altitudes (ELA) for eight Pleistocene glaciers on the Fish Lake Plateau, south-central Utah. Modern ELA levels (4900 m, 6^0 C/1km lapse rate) are estimated from regression to the summer 0° C isotherm with climate data from Loa, Utah (National Climate Data Center, 2007).